BULLETIN OF THE POLISH ACADEMY OF SCIENCES
TECHNICAL SCIENCES, Vol. 74(2), 2026, Article number: e157321
DOI: 10.24425/bpasts.2026.157321

Analysis of the sensor architecture for a level 3 autonomy system in tracked military vehicles

Sebastian JAKUBOWSKI[1,2] **and Jakub WIECH**[3]*

[1] Doctoral School, Rzeszow University of Technology, Powstancow Warszawy 12 st., 35-959 Rzeszow, Poland
[2] Huta Stalowa Wola S.A., gen. Tadeusza Kasprzyckiego 8 st., 37-450 Stalowa Wola, Poland
[3] Faculty of Mechanical Engineering and Aeronautics, Rzeszow University of Technology, Powstancow Warszawy 12 st., 35-959 Rzeszow, Poland

Abstract. The article presents an analysis of the sensor system architecture designed for third-level autonomy in full-scale tracked platforms intended for military applications. In particular, it focuses on the use of advanced data fusion, enabling the integration of information from heterogeneous sensors, such as LiDARs, cameras, ToF (time-of-flight) sensors, inertial measurement units (IMUs), radars, and vehicle on-board systems. This configuration ensures a high degree of environmental perception accuracy and reliability in decision-making, which is crucial under the dynamic and demanding terrain conditions typical of combat operations. It also enhances situational awareness. Key aspects of designing the sensory system are discussed in detail, including the optimal selection of sensors, their placement on the tracked vehicle, and the implementation of real-time data fusion algorithms. The analysis covers the evaluation of these technologies in terms of environmental mapping accuracy, operational reliability, and adaptability under varying operational conditions. The research results indicate that an appropriate sensor architecture, supported by advanced data processing methods, significantly improves the effectiveness of condition-based autonomous control and the vehicle ability to adapt to the specific requirements of combat missions. The conclusions drawn from the study provide valuable guidance in designing modern military vehicles that utilize state-of-the-art sensing technologies and autonomous algorithms.

Keywords: sensor architecture; autonomous tracked vehicle; self-propelled mortar.

1. INTRODUCTION

The development of autonomous systems for military applications has gained significant attention in recent years, driven by advances in artificial intelligence (AI), sensor technologies, and data fusion techniques. Autonomous military vehicles must operate in highly dynamic and often unpredictable environments, requiring a robust sensor architecture to ensure reliable perception, navigation, and decision-making. Among various autonomy levels, Level 3, as classified by the Society of Automotive Engineers (SAE), enables vehicles to perform specific tasks autonomously while still requiring human intervention in complex situations [1]. Special tracked vehicles, such as armored personnel carriers and unmanned combat ground vehicles, leverage such autonomous capabilities to enhance operational efficiency, reduce crew workload, and improve battlefield survivability [2–4]. The development of autonomous control systems for military vehicles constitutes a key element of contemporary research and development efforts in the field of robotics and automation for modern warfare. Heavy tracked platforms, such as the Universal Modular Tracked Platform (UMPG in Polish), require advanced environmental perception systems to effectively execute missions under combat conditions. The analysis focused on the utilization of UMPG as a carrier for the 120 mm RAK 4 Mortar Turret System.

*e-mail: j.wiech@prz.edu.pl

Manuscript submitted 2025-04-18, revised 2025-08-29, initially accepted for publication 2025-11-14, published in March 2026.

One of the primary challenges in implementing Level 3 autonomy in military tracked vehicles is the integration of an advanced sensor suite capable of operating efficiently under extreme conditions, including difficult terrains, limited visibility, and threats associated with electronic warfare. Unlike wheeled platforms, tracked vehicles encounter additional complications, such as increased vibrations, variable traction, and mobility constraints in harsh environments, further complicating sensor performance and data interpretation [5–7]. These challenges must be addressed by an advanced multisensor system that ensures high situational awareness and precise localization.

A robust sensor architecture for autonomous military vehicles typically integrates various sensor modalities, such as LiDAR, radar, cameras, and inertial measurement units (IMUs), enabling comprehensive perception through data fusion techniques. LiDAR provides high-resolution three-dimensional environmental mapping, radar ensures obstacle detection in adverse weather conditions, cameras facilitate object recognition and classification, while IMUs support motion estimation and stability control [8, 9]. Additionally, GPS sensors and odometry enhance localization accuracy, enabling precise maneuvering in environments with GPS signal interference, which is a common challenge in combat scenarios [10, 11].

Data fusion plays a crucial role in improving sensor reliability and accuracy by integrating information from multiple sources and compensating for individual sensor limitations. Various fusion techniques, including Kalman filtering, particle filtering, and deep learning-based approaches, support perception, classification, and trajectory planning [12–19]. These techniques

enable autonomous vehicles to operate effectively by filtering noise, compensating for occlusions, and enhancing real-time decision making.

Recent advancements in artificial intelligence and machine learning have further refined data fusion strategies, enabling adaptive learning, pattern recognition, and anomaly detection in military environments [20–23]. AI-assisted sensor fusion has been shown to significantly improve threat detection, target tracking, and autonomous responses in combat scenarios [24].

Beyond sensor selection and data fusion methods, the autonomous system architecture must also consider aspects related to power consumption, bandwidth limitations, and cybersecurity resilience. Implementing secure communication protocols and resilient sensor networks is essential to counteract threats related to electronic warfare disruptions and cyberattacks on autonomous military platforms [25–27]. Ensuring system redundancy and fail-safe mechanisms is crucial for maintaining operational effectiveness in environments with varying threat levels [28].

The objective of this study is to analyze the sensor architecture necessary for the implementation of Level 3 autonomy in military tracked vehicles, with a particular focus on data fusion methods. The study evaluates available sensor technologies and fusion strategies, allowing for the formulation of recommendations regarding optimal sensor configurations to ensure reliable autonomous vehicle operation in military environments. The developed sensor architecture analysis model can be applied not only to self-propelled mortars but also to other artillery systems and combat vehicles requiring a high degree of autonomy. The results of this research may contribute to enhancing the operational efficiency of autonomous military platforms in dynamic and unpredictable battlefield environments.

2. RESEARCH METHODS

The research study was preceded by an analysis of military standards defining the requirements for military vehicles and autonomous control systems in tracked platforms. Key guidelines derived from NATO STANAG standards, Polish Defense Standards (PNO), and Allied Environmental Conditions and Test Publications (AECTP) were considered. The analysis included standards related to equipment resistance to environmental conditions, including the AECTP-300 standards, which specify requirements for device operation in extreme climatic conditions such as salt fog, smoke, and sudden pressure changes. Additionally, guidelines on resistance to electromagnetic disturbances (PDNO-A-STANAG-4370/AECTP-250) [29], safety in explosive atmospheres (NO-A-STANAG-4370/AECTP-300-16) [30], and resistance to radioactive contamination in accordance with MIL-STD-883 [31] and MIL-STD-810H [32] were reviewed. The scope of the analysis also included guidelines contained in the U.S. MIL-STD-810 standard, which concerns environmental testing of military equipment. The results of this analysis form the basis for assessing the feasibility of implementing autonomous systems in tracked vehicles operating in combat conditions.

As part of the study, environmental conditions and military requirements in the operational area were considered, relating them to the specific tasks performed by the mortar mounted on a tracked platform. Based on a review of military and civilian literature on the autonomy of wheeled and tracked vehicles, potential sensor architectures were analyzed, appropriate sensors were selected, and possible control, processing, and data fusion algorithms were proposed.

3. AUTONOMOUS MOBILE PLATFORM AND ITS REQUIREMENTS

The M120 RAK self-propelled mortar on the UMPG tracked platform is characterized by its ability to overcome water obstacles and operate efficiently in diverse terrain and climatic conditions. The vehicle design ensures crew protection against small arms fire, anti-tank grenade launchers, and explosions from mines and improvised explosive devices. The frontal armor of the hull provides protection at Level 4, while the side armor meets level 3 protection standards according to STANAG 456 [33].

While traversing difficult terrain, the mortar is subjected to vibrations resulting from the propulsion system and movement on tracks, with vibration frequencies averaging 50 Hz for steel tracks and 70 Hz for elastomer tracks at speeds of 50 km/h [34]. These parameters, in accordance with STANAG 4370 (AECTP-400), confirm the system adaptation to operating under intense dynamic loads during combat operations. Additionally, due to the necessity of maintaining the vehicle buoyancy, the autonomy system and additional equipment must have a total weight not exceeding 300 kg. The M120 RAK self-propelled mortar on the UMPG tracked platform is presented in Fig. 1.

Fig. 1. View of the M120 RAK self-propelled mortar on UMPG [35]

3.1. Military requirements

The analysis below has been developed on the basis of the military standards TC 3-22.69, ARN3488, and ATP 3-09.42 [36,37]. A self-propelled mortar is a firepower weapon with a high barrel

elevation angle, relatively short range, and high rate of fire, designed for suppressive fire across wide areas. Its mobility allows it to be used for close support of maneuvers and rapid response. The support company (mortar fire platoon) may carry out the following tactical tasks:

- Engaging enemy combat assets;
- Disrupting enemy combat operations, command, reconnaissance, and supply systems;
- Preventing attacks and blocking maneuvers;
- Providing fire cover for gaps in the combat formation of own troops;
- Providing fire support to engineering obstacles;
- Conducting fire surveillance of areas (enemy approach routes and maneuver corridors);
- Reducing the enemy's fire support potential;
- Demolishing defensive fortifications and other installations;
- Blinding observation systems;
- Harassing the enemy;
- Providing fire cover for the maneuver of own forces;
- Creating disruptions in enemy observation;
- Providing illumination support for operations;
- Designating targets for air forces.

The primary task of the conditional autonomy system for the chassis of the support vehicle is to ensure the mobility of the unit during the execution of tactical missions of the mortar platoon. Driving capabilities must enable rapid and safe movement of the vehicle in a diverse combat environment, while maintaining full operator intervention capability. The system should allow autonomous movement both in urban and open terrain, taking into account roads, off-road areas, as well as natural and artificial obstacles. It must be capable of following a route designated by the commander, as well as dynamically adjusting it depending on situational changes. The chassis should enable rapid deployment to designated operational areas, efficient repositioning during combat operations, and coordinated movement in a column with other vehicles. Of particular importance is maintaining synchronization and appropriate distances between units. A critical requirement is the ability to avoid collisions with other vehicles, terrain obstacles, and personnel. The system must allow emergency stops initiated by the operator. Furthermore, redundancy in key subsystems is required to guarantee operation in the event of partial damage. This ensures that the system requirements are explicitly traceable to the tactical use cases, clarifying how mobility tasks of the mortar platoon translate into concrete design needs for the autonomy system

3.1.1. Basic tasks of the self-propelled mortar

The combat formation of a firing platoon consists of the command point of the platoon commander, mortar firing positions and a waiting position. The command point is intended to develop firing settings, direct fire and maneuver of the platoon. The mortar firing position is a place convenient for taking and conducting indirect, semi-indirect and direct fire. This position is selected by the mortar commander in an array determined by the platoon commander, so as to ensure concealment from enemy reconnaissance. The time the vehicle stays at the firing position should not exceed 2 minutes from the moment of opening fire. The waiting position is a place in the field that is convenient for the deployment of the command vehicle and mortars of the firing platoon, ensuring their concealment and free execution of maneuver to the firing positions and rest. For the support company, the battalion commander designates Artillery Manoeuver Areas (AMA) for the deployment of combat formation elements and the execution of tasks, as well as the area for deploying reconnaissance elements. The parameters of the artillery maneuver areas, such as dimensions, location and distance from the front edge of friendly forces, are established depending on the scope of tasks, the combat formation of the supported fighting forces, terrain conditions and technical capabilities of the means of communication. In order to maximize the survivability of the combat formation elements within the AMA, the distance between its individual parts should be greater than half a kilometer.

In order to adopt a convenient shape of the combat formation and thus achieve readiness to perform fire support tasks, changes in the position of the group elements are carried out, referred to as maneuvers. We distinguish between internal and external maneuvers. An internal maneuver consists in a quick and organized abandonment of the previously occupied firing position or waiting position and taking up another firing position or waiting position within the occupied maneuver area of the fire platoon. In the case of self-propelled mortars, an internal maneuver is performed immediately after completing a fire task in order to avoid losses from enemy firepower. An external maneuver is a quick and organized exit from the previously occupied maneuver area of a support company or platoon and achieving readiness in a new area with a simultaneous change of combat formation. It is carried out in order to adopt the most convenient grouping in relation to the expected scope of tasks, ensure continuity of fire support and maintain survivability.

The implementation of a movement consists in moving troops from one area to another in order to create a planned combat grouping or to concentrate forces. A movement, unlike an external maneuver, includes marching and transporting subunits. It can be carried out using own means as well as rail, sea, air or combined transport.

A march is a movement of troops organized in marching columns on roads or cross-country. Its purpose is to reach a designated area while maintaining the ability to carry out combat tasks. In order to carry out a march, units are formed into a marching column with appropriate parameters. In order to efficiently manage the march, the starting points, coordination points and exits from the route are determined, as well as the times of their passage. The march is carried out in the so-called march grouping, which ensures the timely execution of the march, efficient development of the sub-unit into a combat grouping in order to support the sub-units, freedom of movement and maintaining the continuity of command.

The mission profile of the support company, including the mortar platoon, focuses on providing fire support through disrupting enemy operations, protecting friendly forces, and block-

ing adversary maneuvers. Mobility plays a key role in carrying out these tasks, enabling rapid occupation and relocation of positions, as well as coordination with other units. Consequently, the vehicle chassis conditional autonomy system must support the ability to maneuver effectively across diverse terrain under dynamically changing tactical conditions. The primary challenges include ensuring reliable positioning in the event of navigation system disruptions, safely avoiding natural and artificial obstacles [38], and maintaining interoperability within the formation. Another critical issue is resilience to communication interference and the operator's ability to immediately assume control. Ultimately, the system effectiveness is determined by its capacity to combine autonomous mobility with the requirements of safety and full human control.

3.2. Autonomous driving problems

Autonomous navigation in rough and natural terrain faces many more challenges than navigation on structured roads. One of the central problems is localization and perception. Visual odometry (VO) and simultaneous localization and mapping (SLAM) are widely used for estimating the position of unmanned ground vehicles. However, these techniques often fail in off-road environments. A major issue is drift, which means that small errors in position estimation add up over time and can cause large deviations from the real path. Another problem is scale error in monocular systems, where the vehicle does not know the true depth of the environment without additional sensors. In terrain covered by grass, bushes, or rocks, the visual features are often repetitive or weak, which makes it difficult for algorithms to find stable keypoints. Environmental conditions further complicate this task: changing illumination, shadows, rain, fog, and dust reduce image quality and make matching unstable. On moving vehicles, motion blur and rolling shutter effects create further challenges. Solutions found in the literature include using stereo or visual–inertial pipelines to recover scale and reduce drift, applying robust methods such as RANSAC and bundle adjustment to filter out outliers, and employing loop closure to correct accumulated errors. Researchers also recommend using multi-camera systems that cover a wider field of view and increase the chance of finding reliable features in natural scenes [39, 40].

Apart from technical perception challenges, there are system-level problems that strongly influence the deployment of autonomous vehicles. Safety validation is one of the most discussed barriers, since it is difficult to prove that a system will remain reliable under all possible conditions in unstructured terrain. Cybersecurity is another serious risk, since unmanned vehicles rely on large amounts of sensor data and communications that can be attacked or disrupted. In addition, infrastructure is often not ready to support autonomous vehicles in rural or military contexts, especially when there is no high-quality digital map or stable communication. Suggested solutions include carrying out pilot programs to collect safety evidence step by step, defining clear standards for testing and evaluation, creating legal frameworks for liability and insurance, and promoting data sharing agreements between industry and regulators. Although most of these discussions started in the context of road vehicles, they also apply to military and off-road robots, where reliability under degraded conditions is even more important [41].

For tracked vehicles and off-road ground robots, there are additional difficulties related to their mobility and odometry. Tracked platforms often experience slip and skid, which means that the movement of the tracks does not match the actual displacement of the vehicle. This creates systematic errors in odometry and can seriously affect localization when GNSS is weak or unavailable. Another critical issue is negative obstacles, such as ditches, trenches, or drop-offs, which are especially dangerous because they may not be visible to sensors mounted high on the vehicle. These obstacles appear as empty space, which can be hard to detect with standard LiDAR scanning horizontally. Researchers have worked on solutions such as tilted or low-mounted LiDARs that reduce blind spots close to the ground, and sensor fusion techniques that combine LiDAR, vision, and IMUs to provide continuous localization even without GNSS [42, 43].

Another class of problems comes from mobility in difficult terrain. Tracked vehicles are well-suited for off-road navigation, but they consume much energy and their mechanical parts are exposed to high wear when moving in mud, sand, or over rocks. On steep slopes, the risk of slip is high and the power demand increases. Vibrations generated during motion also reduce the performance of sensors such as cameras and LiDARs, which need stable mounting to work correctly. In the literature, solutions include adaptive suspension systems that change their stiffness or damping depending on the terrain, terrain-aware path planning that selects routes with lower risk of slip or rollover, and slip estimation models that adapt driving commands to soil and track interaction [44].

Finally, environmental and operational conditions play a major role in the success of off-road autonomy. Many sensors degrade in dust, rain, fog, or under dense vegetation. For example, cameras may be blinded by mud or low light, while LiDAR performance can be reduced by fog and dust. Long missions require heavy energy consumption for sensing and computing, which produces heat and demands robust power management. Overheating is especially problematic in military or desert environments. Literature on defense-oriented vehicles underlines the importance of system reliability: redundant sensors ensure that perception continues even if one modality fails, fail-safe control layers prevent loss of control during software faults, and robust communication links secure coordination between multiple unmanned systems. These principles show that advances in off-road autonomy depend not only on better algorithms, but also on robust vehicle design and integration of redundancy across hardware and software [45, 46].

3.3. Sensor requirements

The autonomy system of the vehicle must include a sensor suite capable of performing all specified mobility operations at a level no less effective than a human driver. Additionally, it should enhance situational awareness, thereby providing added value to the driver's functions and improving the combat effective-

ness of the unit. A Level 3 autonomy system can significantly increase the platform's capability to operate in unmanned or assisted modes, reducing operator workload, extending operational marching periods, and enhancing mission effectiveness.

In this paper, situational awareness is defined as a continuous understanding of the near and mid-field environment so that speed, steering, and braking actions are timely and appropriate. The autonomous controller takes the role of that driver: it must maintain a clear forward preview, and retain reliable perception in darkness, dust, rain, fog, and glare. The fused perception must support safe stopping at the current speed, obstacle avoidance in tight spaces, and stable alignment when entering or exiting narrow routes or ramps. In short, the human driver's situational-awareness standard is used as a design target, but the autonomous controller is the "driver" that achieves it through sensing, fusion, and planning.

Translating this baseline into minimum necessary capabilities, the system should provide wide field-of-view coverage for close-range context, a forward look for longer-range preview, and a range-capable modality (radar or LiDAR) that gives dependable distance cues when visual contrast is poor. Time stamping and synchronization stabilize the perception against vibration and motion, while the autonomy stack consumes these data to compute safe margins, recommended speeds, and collision-free trajectories.

The requirements for the tasks and behavior of a tracked vehicle encompass both general sensor selection criteria and autonomous behaviors, in accordance with military requirements. The sensor system should facilitate easy replacement and integration of new modules, increasing its adaptability to changing operational conditions. Sensors must support autonomous behaviors such as convoy following in peacetime, precise maneuvering to a commander-designated BCT or headquarters point with an accuracy of ±5 meters, vehicle orientation adjustments, and trajectory tracking. All these functions require advanced data fusion from cameras, LiDARs, radars, and inertial navigation systems.

Selected sensors for the autonomy system must coexist with previously implemented military vehicle systems and should not pose a risk to operations. Active sensors based on laser technology may not only interfere with laser illumination detection systems, such as self-defense or targeting apparatus, but also reveal vehicle positions due to visible beams in night vision, disrupting targeting and panoramic observation instruments. The self-defense system of the vehicle, SSP-1 OBRA-3, which detects radiation in the wavelength range of 600 nm to 11 000 nm [47], has been analyzed. The most commonly used LiDARs and time-of-flight (ToF) sensors operate in the 900 nm to 1550 nm range, overlapping with the detection range of SSP-1 OBRA-3 [48]. Specialized LiDAR solutions exist with wavelength ranges up to 10 000 nm, which also fall within the detection range of the optoelectronic heads of the discussed system and may interfere with self-defense operations of the vehicle or cause unwarranted firing of system effectors [49]. This issue affects not only the vehicle implementing the sensory system but also accompanying vehicles equipped with similar systems.

4. ENVIRONMENTAL AND CLIMATE CONDITIONS

Military vehicles, and consequently the sensors installed on them, must be adapted to the environments in which they operate. These conditions can be categorized into natural conditions, which result from the characteristics of the natural environment and climate where the vehicle operates, and combat conditions, which occur during field exercises and armed conflicts. Natural conditions include atmospheric conditions and terrain characteristics, while combat conditions involve the presence of smoke, dust, explosions, vibrations, and electromagnetic interference, all of which can affect sensor performance.
For the purpose of further analysis, it is assumed that the analyzed tracked vehicle will operate in a temperate environment.

4.1. Climate and natural environment

The analysis of climatic and environmental conditions was conducted using data from The Climate Change Knowledge Portal [50] and the Copernicus Climate Change Service [51], as well as scientific publications describing conditions in temperate environments [52–55]. Additionally, the military standard STANAG 4370, which outlines environmental requirements for autonomous equipment, was considered.

A temperate environment is characterized by significant variability in climatic conditions and terrain features, posing challenges for autonomous systems. The climate in regions classified as temperate is influenced by both oceanic and continental factors, resulting in considerable fluctuations in temperature and precipitation. Lowland areas exhibit moderate temperatures, with winter periods ranging from approximately -2°C to -5°C and summer temperatures between 18°C and 25°C, with occasional extreme heat waves exceeding 35°C. In contrast, mountainous regions experience harsher conditions, with winter temperatures dropping below -10°C and summer temperatures ranging between 10°C and 15°C. Annual precipitation totals vary depending on topography, from approximately 500 mm in lowland areas to over 1500 mm in mountainous regions, with peak precipitation occurring in summer due to convective storms. Climate change models project an increase in average temperatures by 2–4°C over the next 30–50 years, leading to shorter and milder winters, extended summer periods, and intensified extreme weather events. These changes include increased winter precipitation and decreased summer precipitation, which can increase the risks of droughts, extreme heat waves, and flash floods.

The diversity of the studied terrain includes lowland, upland, mountainous, marshy, forested, and river valley regions, each requiring specific technological adaptations. Lowland areas have loose soils that become dry and dusty in summer and muddy in transitional periods. Upland regions present a more varied topography, with steep slopes, rocks, and intense erosion processes, complicating navigation. Mountainous areas undergo dynamic environmental changes. Winter is dominated by snowfall and ice, spring may bring landslides, and summer presents challenges related to muddy trails and rapid water flows. Marshy areas are characterized by unstable ground, especially during thaw periods, whereas forested regions contain natural obsta-

cles such as fallen trees, dense vegetation, and muddy paths. River valleys are susceptible to periodic flooding and sediment deposition, altering the terrain structure.

4.2. Military environmental conditions

Autonomous ground vehicles intended for military missions must tolerate broad climatic envelopes in routine operation. Operating temperatures of -20°C to +50°C with relative humidity up to 95 % are consistent with NATO STANAG 4370 (AECTP-200, Environmental Conditions) and the corresponding verification methods in MIL-STD-810H (high/low temperature: Methods 501/502, humidity: Method 507), which are the baseline documents used to derive requirements and laboratory profiles for land systems [32, 56, 57]. In addition to climatic stresses, off-road vehicles experience sand and dust, vehicle-grade vibration, and mechanical shock. These exposures are characterized in AECTP-300/400 (climatic and mechanical test families) and verified using MIL-STD-810H procedures (sand and dust: Method 510, vibration: Method 514, shock: Method 516) that reflect rugged-terrain usage [32, 57].

Ingress and water protection follow international and military practice. IEC 60529 defines IP65 (dust-tight and water jets) and IP67 (dust-tight and temporary immersion to 1 m for 30 min) classifications for exposed electronics such as onboard sensors [58]. When platforms have amphibious or deep-fording roles, sealing is further demonstrated via MIL-STD-810H Method 512 (Immersion) and service test procedures for vehicles (e.g., U.S. Army TOP 2-2-612, Fording), which directly link enclosure protection to amphibious mission needs [32, 59].

Outdoor illumination encountered by imaging sensors spans $\approx$ 1 lx (civil-twilight order) up to $\approx$ 50 000 lx (bright daylight), a conservative subset of well-documented ranges that place clear-sun conditions near 10^5 lx and nighttime/twilight at single-lux or lower levels. This envelope is supported by International Commission on Illumination (CIE) daylight/sky documents and all-weather sky illuminance modeling in the lighting literature [60, 61]. Low-visibility phenomena (fog, heavy rain, snow/icing) are an expected part of mission environments. AECTP-200 and associated leaflets (e.g., AECTP-230) enumerate these climatic conditions, and AECTP-300 provides the corresponding test methods (rain, icing/freezing rain, solar radiation) used to specify and verify operation in degraded visibility [56, 57, 62].

Detection-range expectations for perception sensors in unstructured terrain are grounded in off-road literature. In the DARPA desert environment, Thrun *et al*. report near-field obstacle detection by laser scanners on the order of tens of meters ($\approx$ 22 m) and vision-based drivable-terrain perception beyond 70 m at highway speeds, illustrating the longer look-ahead of cameras when contrast is favorable [45]. Heavy off-road systems such as CMU Crusher employed multiple ladar units, a widely used scanner of that era, the SICK LMS-291, specifies 0–80 m maximum range ($\approx$ 30 m at 10% reflectivity) with IP65 enclosure—figures consistent with 0.5–100 m design bands for lidar in mixed off-road scenes [63, 64]. For radar, classic off-road experiments by Matthies *et al*. show detection of a large tree trunk behind 2.5 m of dense foliage, highlighting radar utility through vegetation where optical/laser sensing attenuates [65]. Recent field work on radar-only off-road navigation demonstrates successful multi-hundred-meter traverses and a range advantage under adverse conditions, supporting minimum ranges of $\geq$ 50 m in degraded visibility for radar and design ranges on the order of 0.5–100 m in moderate conditions [66]. Taken together, these sources justify specifying mid-to-long look-ahead for camera systems in good conditions, 0.5–100 m for lidar/radar in routine off-road operation, and conservative minima under severe weather of $\geq$ 50 m (radar), $\geq$ 50 m (lidar), and $\approx$ 25 m (camera) [45, 63–66].

For high-severity deployments, an extreme environmental envelope of –40°C to +70°C, IP67 immersion, and operation under fog, heavy rain, and snow/icing is consistent with AECTP-200 climatic categories and the verification methods of AECTP-300 and MIL-STD-810H (low/high temperature, rain and icing/freezing rain, immersion) [32, 56, 57, 59].

Changing climate conditions increase demands on sensor technology, particularly in mountainous and southern regions, where the risks of droughts, extreme precipitation, and dust storms are rising. In these environments, sensor reliability and adaptability are critical to ensuring the safety and effectiveness of autonomous off-road vehicles. A summary of the climate and environmental analysis is presented in Table 1.

4.3. Operational conditions

The support vehicle with a conditional autonomy system avoids moving along roads in order to minimize the risk of detection and engagement by the enemy. It is expected to cover distances ranging from several to over a dozen kilometers within a single operational cycle, with frequent position changes required by the nature of mortar platoon missions. The area of operation consists mainly of off-road terrain, forested areas, open fields, and uneven ground with natural obstacles such as hills, ditches, or watercourses.

The intensity of maneuvering will be high, as the vehicle must dynamically respond to changes in the tactical situation while avoiding predictable movement routes. Under combat conditions, the availability of objects that could aid localization, such as buildings, power lines, or topographic landmarks, is limited and often incidental. Therefore, the system should be designed to operate in an environment with incomplete navigation infrastructure, relying primarily on onboard sensors and interference-resistant data integration. Only occasional terrain features or artificial structures may provide additional support for improving localization in critical situations.

During operational activities, a tracked vehicle is exposed to a wide range of destructive factors resulting from explosions, gunfire, and extreme environmental conditions. Military standards such as STANAG 4370 (AECTP-300, AECTP-400) define the resistance requirements for the vehicle and its sensory systems to phenomena associated with operational engagements. The analysis covers the impact of shock waves, overloads, pressure changes, and resistance to chemical, radiological, and electromagnetic factors.

One of the key combat factors is the shock wave generated during explosive detonations. The assumed resistance is to an

Table 1
Summary of operational conditions for the self-propelled mortar sensor system in a natural environment

Category	Moderate requirements	High requirements	Standard / Method
Operating temperature	–20°C to +50°C	–40°C to +70°C	AECTP-200, MIL-STD-810H (Methods 501/502)
Relative humidity	Up to 95%	Up to 100%	AECTP-200, MIL-STD-810H (Method 507)
Protection rating (IP)	IP65	IP67	IEC 60529, MIL-STD-810H (Method 512)
Lighting	1 lx (twilight) to 50,000 lx	0 lx to 100,000 lx	CIE S 011/E, all-weather sky model [61]
Detection range (LiDAR, radar)	0.5 m to 100 m	0.5 m to 200 m	Off-road literature: [63–66]
Detection range (camera)	Up to 50 m	Up to 80 m	Off-road literature: [45], manufacturer requirements
Dust and mud resistance	Dust and mud contamination	Full resistance	AECTP-300, MIL-STD-810H (Method 510)
Vibration resistance	Vibrations on unpaved roads	Vibrations in rocky terrain	AECTP-400, MIL-STD-810H (Methods 514, 516)
Water resistance	Water jets	Submersion up to 1 m	IEC 60529, MIL-STD-810H (Method 512)
Operation in low visibility	Fog, light rain	Fog, heavy rain, snow	AECTP-230, AECTP-300

explosion of 3 kg of TNT at a distance of 3 meters. Based on Brode's formula, it has been calculated that such an explosion generates an overpressure of 0.36 MPa (3.6 bar), which can cause severe structural and electronic system damage. Furthermore, during mortar firing from the tracked platform, the vehicle is subjected to sudden pressure changes. According to AECTP-400 (STANAG 4370), the pressure changes depending on the distance from the muzzle are as follows: 22.2 kPa (0.22 bar) at 3 m, 12.5 kPa (0.125 bar) at 4 m, and 8 kPa (0.08 bar) at 5 m. Additionally, during firing, accelerations reaching up to 561 g occur, imposing high demands on stabilization and sensor protection systems.

In addition to shock wave impact and overload, the vehicle must demonstrate resistance to extreme environmental conditions as per AECTP-300. This includes survival in acidic and saline environments (pH 1.67 for 2 hours at 35°C) and resistance to salt fog with a 5% NaCl concentration for at least 24 hours. In explosive atmospheres (AECTP-300-16:2022), equipment enclosures must not exceed a temperature of 223°C to prevent the ignition of n-hexane. Furthermore, according to KCS-05 standards, electronic systems must be resistant to electromagnetic interference (EMI), which could disrupt the operation of the sensor and communication systems. The vehicle must also comply with radiation contamination resistance standards as specified by MIL-STD-883 or MIL-STD-810H. A summary of the combat and design conditions for the tracked vehicle is presented in Table 2.

5. DATA FUSION IN AUTONOMOUS TRACKED VEHICLE SYSTEMS

Data fusion in autonomous tracked vehicle systems is the process of integrating information from various sensors to obtain a coherent environmental representation. This process is essential for effective navigation, obstacle detection, and real-time decision making. In a combat environment, where conditions are dynamic and unpredictable, data fusion enhances system reliability and operational safety.

The requirements for sensors in the context of data fusion go beyond their basic technical parameters, which were previously considered in the environmental and combat analysis. Temporal synchronization of data from different sources is necessary, requiring the implementation of reference clocks and delay correction mechanisms. Sensors must be compatible in terms of sampling frequency and the data processing system must be able to approximate sensory data in the event of temporary connection loss or active interference attempts. Ensuring adequate spatial and temporal resolution is also crucial for accurately analyzing the dynamically changing environment.

Sensor architecture includes data processing at three levels: raw data, feature extraction, and decision-making. Fusion at the raw data level allows for the direct combination of measurements from various sensors in their original form, enabling early detection of inconsistencies and anomalies. At the feature extraction level, the system identifies relevant information, such as object contours or movement directions, integrating data with similar characteristics. Decision-level fusion involves combining processed results from individual sensors to make final decisions about navigation or responses to environmental changes.

Various data fusion algorithms are employed in practice, including Kalman filters, especially the extended Kalman filter (EKF) and unscented Kalman filter (UKF) [67], which estimate the vehicle's state based on uncertain and noisy measurements. Graph-based algorithms facilitate modeling spatial relationships between objects [68], while neural networks are used in visual data analysis and object trajectory prediction.

Table 2
Summary of combat and design conditions for the tracked vehicle

Category	Requirement	Standard / Method
Shock wave and pressure changes		
Overpresscre from shock wave (3 kg TNT, 3 m)	0.36 MPa (3.6 bar)	Calculations based on Brode's formula
Pressure changes during firing (3 m)	22.2 kPa (0.22 bar)	AECTP-400
Pressure changes during firing (4 m)	12.5 kPa (0.125 bar)	AECTP-400
Pressure changes during firing (5 m)	8 kPa (0.08 bar)	AECTP-400
Overloads after firing	Up to 561 g	AECTP-400
Environmental conditions		
Resistance to acidic/saline environment	pH 1.67, 2h, 35°C	AECTP-300 (Methods 309, 314, 319)
Resistance to salt fog	5% NaCl, 24h, 35°C	AECTP-300-9
Relative humidity	Up to 100%	AECTP-300
Operating temperature range	–40°C to +70°C	AECTP-300
Full submersion resistance	IP67	AECTP-300
Protection against dust and mud	IP67	AECTP-300
Combat and radiation hazards		
resistance to electromagnetic interference (EMI)	Compliance with EMC requirements	PDNO-A-STANAG-4370/AECTP-250
Resistance to explosive atmosphere	Max. enclosure temperature: 223°C	AECTP-300-16:2022
Resistance to radioactive contamination	Compliant with MIL-STD-883 or MIL-STD-810H	MIL-STD-883, MIL-STD-810H
Design conditions		
Vibrations from track system (steel)	50 Hz	AECTP-400
Vibrations from track system (elastomeric)	70 Hz	AECTP-400
Maximum autonomy system weight	Up to 300 kg (to maintain buoyancy)	Manufacturer requirements

Implementing data fusion in tracked vehicles presents multiple challenges, such as synchronizing data from sensors with different architectures and operating frequencies, noise elimination, and adapting algorithms to changing environmental conditions. The system effectiveness depends on precise sensor calibration, their placement on the vehicle, and the application of real-time processing algorithms.

In the case of Kalman filtering, particularly its EKF and UKF variants, additional data filtering methods can be applied to increase system reliability. Despite its higher computational complexity, the particle filter enables effective state estimation in nonlinear dynamics and non-Gaussian error distributions [69]. Meanwhile, the median filter helps eliminate isolated measurement errors in vision-based data and time-of-flight (ToF) sensors [70]. Adaptive filters [71] dynamically adjust filter parameters to changing environmental conditions, which is particularly beneficial in highly variable environments.

Ensuring data consistency requires mechanisms that evaluate the coherence of information from different sensors. Consistency-oriented data fusion in distributed multisensor systems [72] involves analyzing and comparing measurement results from various potentially correlated sources to detect inconsistencies, anomalies, or errors in data. Predictive model-based algorithms use historical data and vehicle dynamics models to assess whether obtained results align with expected values. Examples of such mechanisms include correlation analysis of sensors with different characteristics, such as LiDAR and camera [73], as well as statistical deviation detection algorithms [74]. Additionally, threshold-based systems enable immediate identification of erroneous data by establishing permissible deviation limits, such as error detection through residual distribution analysis in Kalman estimation.

6. POTENTIAL CONTROL AND DATA PROCESSING ALGORITHMS

Control and data processing algorithms in an autonomous tracked vehicle can be categorized into three areas: perception, data fusion, and navigation. In perception, neural networks can be employed for image segmentation (e.g., DeepLabV3+ [75] or vision transformers [76]) to distinguish terrain classes such as mud, water, or sand. Furthermore, single-pass object detection models (such as YOLOv8 [77]) can facilitate the early detection of potential threats, including people, animals, or large obstacles. With such real-time analysis, the vehicle can gain a detailed understanding of its environment and react instantly to changes. Simultaneously, combining deep depth estimation networks (such as DPT [78]) with LiDAR or radar measurements can ensure a more accurate 3D model of the surroundings.

The next step involves data fusion within the SLAM (simultaneous localization and mapping) module. Algorithms such as GraphSLAM [79] or particle filter-based approaches [80] can

integrate different measurement types (images, point clouds, radar signals) into a coherent environmental model. The resulting localization and mapping information can then be utilized for global path planning using methods like Hybrid A* [81] or D* Lite [82]. For local obstacle avoidance, algorithms such as dynamic window approach (DWA) [83] can enable reactive trajectory adjustments. To ensure smooth track control while considering terrain factors (e.g., slipping in mud), techniques such as model predictive control (MPC) [84] or reinforcement learning (e.g., PPO [85]) can be implemented to dynamically learn optimal movement strategies under various conditions.

Assuming a maximum vehicle speed of approximately 65 km/h, key factors include data refresh rate and sensor range. Cameras should operate at a minimum of 25–30 frames per second (FPS) to allow object detection and segmentation algorithms to effectively track environmental changes. A sufficient resolution (e.g., Full HD) ensures high obstacle recognition accuracy but must be supported by adequate communication link (e.g., gigabit Ethernet or fiber optics) and a computational unit capable of processing large data streams in real time.

LiDAR should provide a scanning frequency of at least 10–20 Hz [86], generating updated point clouds every 50–100 ms, enabling synchronization with approximately every second camera frame. This ensures that the vehicle can detect emerging obstacles in time to react (braking or maneuvering). The LiDAR scanning range should reach 100–150 meters, depending on terrain conditions, providing an AI-based control system with a sufficient planning horizon. Radar, which further assists in detecting moving objects in all weather conditions and lighting scenarios, should offer a range of at least several dozen meters (e.g., 100 m) and an angular resolution that allows distinguishing obstacles on adjacent lanes or near the planned trajectory.

In case of depth sensors (e.g., ToF), measurement frequency should be at least 30 FPS to maintain smooth integration with camera images. Given the vehicle high speed, time synchronization (timestamping) among all devices is critical. Minor delays can lead to incorrect object positioning in the map and reduced response accuracy. Additionally, sensor mounting and calibration must account for terrain-induced tilts and vibrations to maintain observation consistency at high speeds (65 km/h in varied terrain). This ensures that the perception and motion planning system maintains a safety margin when detecting obstacles and executing maneuvers, minimizing collision risks.

7. SENSOR EVALUATION CRITERIA

Sensors must provide the autonomous controller with a situational picture at least equivalent to that required by a skilled human driver. The criteria below, based on literature review, translate this objective into measurable requirements for stopping distance, timing, coverage, and robustness. They are tailored to tracked, off-road operation—where vibration, dust, and poor visibility are prevalent and include criteria necessary for reliable data fusion.

1. **Forward recognition range**
   Must satisfy the stopping rule at design speeds: Road 65 km/h, Off-road 40 km/h .
2. **Time processing**
   Bounds for the decision loop time to < 350 ms.
3. **Field of view (FOV) and angular detail**
   Forward horizontal FOV: $\geq 120°$, vertical FOV: $\geq 60°$.
4. **Range/depth accuracy**
   - LiDAR/ToF range accuracy: $\leq \pm 5$ cm (near to mid range).
   - Radar range resolution: ≤ 0.3 m.
   - Stereo depth error: $\leq 10\%$ at 20 m (or better).
5. **Low-visibility robustness**
   - Night/fog/rain/dust: maintained $R_{\min} \geq 50$ m.
   - Glare/back-lighting: dynamic range sufficient to avoid loss of detections in forward arc.
6. **Coverage and occlusions**
   - Forward view to the $R_{\min}$ target without structural occlusion.
7. **Cybersecurity and integrity**
   Secure data links according to the military requirements.
8. **Environmental hardening**
   - Temperature: $-40°$C to $+70°$C. Humidity: up to 100%.
   - Ingress: IP67 (dust-tight, immersion).
   - Shock/vibration and EMC: comply with applicable military test methods used elsewhere in the paper.
9. **Interference and signature**
   - No interference with onboard protection (e.g., laser warning receivers).

8. SENSOR REVIEW

There are numerous sensors available on the market tailored for autonomous vehicle applications. The following brief review considers the previously presented analysis of sensor operating conditions and the requirements imposed on autonomous off-road vehicles operating in combat conditions.

8.1. LiDARs

The most popular sensor used in mobile robotics is LiDAR, which provides high-quality data on distance and environmental structure by emitting a laser beam and measuring its return time after reflection from an obstacle. LiDAR enables the creation of detailed 2D and 3D maps, which makes it particularly useful for navigation, obstacle avoidance, and localization in unknown or dynamically changing environments. Its independence from lighting conditions makes it an effective tool for outdoor applications, especially in low-visibility conditions. Combined with SLAM algorithms, LiDAR allows for efficient real-time mapping and updating, which is fundamental for autonomous mobility in field robotics.

One of the companies producing LiDARs is Ouster. Their products offer high resolution and reliability in robotics, automotive, and infrastructure applications. The company utilizes digital photonic integrated circuit (Digital LIDAR) technology, ensuring precise environmental mapping. Ouster LiDARs are

distinguished by their compact design, resistance to environmental conditions, and easy integration with ROS-based systems. An example is OS2 LiDAR [87], which offers a detection range of up to 400 m, a vertical resolution of up to 128 channels, a horizontal resolution of up to 2048 points, and a rotation frequency of 10 or 20 Hz, providing over 2.6 million points per second. The device includes an integrated IMU module (InvenSense ICM-20948) with a 3-axis gyroscope and accelerometer, delivering spatial orientation data with a delay of less than 10 ms. The LiDAR communicates via UDP over gigabit Ethernet, operates in a temperature range of -20°C to +60°C, and meets IP68/IP69K standards.

An alternative to Ouster is Velodyne LIDAR, a leader in producing rotating LiDARs widely used in autonomous vehicles, robotics, and infrastructure monitoring systems. The company offers high-resolution models such as the Ultra Puck VLP-32C series [88], featuring 32 measurement channels, a detection range of up to 200 m, and a distance measurement accuracy of ±3 cm. The device generates up to 1.2 million points per second in dual-return mode, with a horizontal angular resolution from 0.1°to 0.4°and a vertical resolution of 0.33°, covering a 360°horizontal and 40°vertical field of view. The LiDAR communicates via a 100 Mbps Ethernet interface, transmitting distance, reflectivity, and time-of-flight pulse data. It operates in temperatures from –20°C to +60°C, has an IP67 protection rating, and uses an eye-safe laser beam with a wavelength of 903 nm.

8.2. Cameras

The next most commonly used sensor in autonomous vehicles is cameras. Cameras can be adapted to operate in different electromagnetic spectrum bands, including visible light, near-infrared (NIR), and far-infrared (FIR). The diversity of these bands allows for image capture in daytime and nighttime conditions, as well as in adverse weather conditions such as fog or rain.

High-resolution cameras aid object recognition, which is crucial for navigation and decision-making tasks. When combined with other sensors such as LiDAR and radar, cameras enhance data fusion, providing a more complete and accurate representation of the vehicle surroundings. The most useful solution are stereoscopic cameras, enabling easy determination of image depth, object distances, and sizes.

A company called Stereolabs offers ZED X series cameras [89], designed for operation in all weather conditions, making them a suitable choice for autonomous robots and machines of various sizes. The ZED X camera features a color sensor with a 1200p resolution at 60 FPS, an advanced Neural Depth Gen2 system for precise depth mapping in the range of 0.3 to 35 m, a vibration-resistant IMU module, a secure GMSL2 connector, an industrial-grade IP67-rated housing, multi-camera synchronization capability, and compatibility with ZED Box devices and GMSL2 cards.

Another interesting manufacturer of cameras for military applications is Etronika. Etronika supplies a wide range of sensory systems for military vehicles, including thermal cameras, night vision systems, laser rangefinders, and observation-targeting instruments. These solutions enable detection, identification, and tracking of objects in various terrain and atmospheric conditions, supporting crew situational awareness. The Etronika FL-KTD-60 camera [90] is an observation device equipped with a thermal and daytime module, consisting of two cameras with a field of view of 60°. The daytime module uses a CMOS sensor with a 1920×1080 px resolution, while the thermal module is based on an uncooled bolometric detector with a 640×480 px resolution, a spectral range of 8–12 µm, and a sensitivity below 50 mK. The camera offers 2× and 4× digital zoom and various IR image color schemes such as “white hot” and “black hot.” The image is transmitted independently for both modules in PAL format or via Ethernet as an H.264 stream, with control via an RS-485 interface. The device operates at temperatures –30°C to +50°C, has an IP67 protection rating, and has heated windows, allowing operation in harsh environmental conditions.

8.3. Radars

Radars are commonly used in civilian vehicles, particularly in passenger cars and trucks, where they support ADAS systems, cruise control, and emergency braking systems. While they can also be applied in military vehicles, it is important to note that radar signals are relatively easy to detect by targeting systems. For this reason, radars are used less frequently in autonomous military vehicles. In the automotive sector, two notable companies offering radar solutions are Aptiv and ZF.

Aptiv’s SRR7 radar [91] is a compact corner sensor designed for detecting objects at close range, with a maximum detection range of 160 m, allowing effective recognition of even motorcycles. It features a resolution of 0.2 m and velocity measurement accuracy of ±0.1 m/s, with a resolution of 0.13 m/s. The radar offers an azimuth coverage angle of ±75° with object differentiation precision of 6°, as well as a vertical coverage angle of ±15°. The device is equipped with a communication interface supporting data transfer rates of 100 Mbps and 1 Gbps.

Another example is ZF’s AC1000T radar [92], a 77 GHz medium-range sensor designed for commercial vehicles, offering a detection range of up to 200 meters and a field of view of 70°, supporting functions such as adaptive cruise control, collision warning, and automatic emergency braking.

8.4. IMU

To determine the position and orientation of a tracked vehicle, inertial measurement units (IMUs) can be used, which measure linear accelerations and angular velocities across three axes. IMUs consist of accelerometers, gyroscopes, and sometimes magnetometers, enabling precise tracking of position, orientation, and vehicle motion in real time. In tracked vehicles operating in diverse and often difficult terrains, IMUs play a crucial role in navigation when GPS signals are unavailable, such as in forests or underground environments. When combined with other sensors like cameras, LiDARs, and radars, IMUs assist localization, stabilization, and trajectory control systems, which are essential for autonomous steering and maneuvering in dynamically changing environments.

An example of an IMU solution provider is Honeywell with its TALIN series, specifically the TALIN 1000 model [93]. This

device integrates GNSS technology, providing orientation accuracy with an error margin of no more than 5 mil RMS and horizontal positioning accuracy of 0.7% of the distance traveled. The vertical positioning error is 0.4%, while the accuracy of the tilt and inclination measurement is 2 mil RMS. The TALIN 1000 is equipped with Ethernet and RS-422 interfaces, supports GNSS receivers, and operates with a power consumption of less than 20 W.

Another company offering similar solutions is AnelloPhotonics with its Anello IMU+ [94]. This inertial measurement unit features a gyroscope with a measurement range of ±200°/s, an angular drift of 0.05°/hr, and a bias stability of 0.5°/hr. The accelerometer offers a measurement range of 8g, bias instability of 20 µg, and a random velocity error of 0.03 m/s/hr. The device operates in temperatures from –40°C to +70°C, withstands accelerations up to 40g, and vibrations of 5g RMS. The IMU+ provides a sampling frequency of 200 Hz with synchronization capability via PPS signals.

8.5. ToF

Time-of-flight (ToF) sensors measure the time it takes for a light pulse to travel to an object and return to the sensor, allowing for distance measurement to surrounding objects. Their operation is based on the emission and detection of infrared light, making them particularly effective for short-range measurements and applications that require a high data refresh rate.

In the context of autonomous military vehicles, the usefulness of ToF sensors is limited. Their range is relatively short, making it ineffective in detecting obstacles at greater distances than required for off-road navigation. In addition, infrared radiation can easily be disrupted by atmospheric conditions such as fog, rain, dust, or smoke, significantly reducing the reliability of the acquired data. In combat environments, the infrared light emission from ToF sensors may also reveal the vehicle position, making it an easy target for adversaries and potentially interfering with other onboard systems and accompanying vehicles. For these reasons, ToF sensors are rarely used in advanced military navigation systems, where LiDARs, radars, and stereoscopic cameras prove to be more effective. It is worth noting that LiDAR, due to its operating principle, can be classified as a ToF sensor.

An example of a simpler LiDAR is the Single-Point Lidar TFS20-L from Benewake. The Benewake TFS20-L [95] is a miniature, single-point ToF LiDAR sensor designed for distance measurement in the range of 0.2 to 20 meters. The device is highly resistant to ambient light up to 100k lx and offers a measurement accuracy of ±6 cm for distances from 0.2 to 6 meters.

8.6. GNSS

GNSS systems such as GPS, GLONASS, Galileo, and BeiDou are widely used for positioning in civilian and commercial applications, typically offering meter-level accuracy or even centimeter-level accuracy when using RTK corrections. In military contexts, especially within 20–50 km of the front lines, GNSS signals are often jammed or spoofed, making them unreliable or entirely unavailable. This necessitates alternative navigation methods.

Table 3 presents a summary of the sensors discussed along with their key parameters. Recognition range for cameras in the table is computed for a vehicle-class target of 1 m width requiring ≈15 px across (daylight), using the pinhole/GSD relation. Other sensors list their vendor detection range.

9. SENSOR ARCHITECTURE

In research on off-road unmanned ground vehicles (UGVs), including military platforms, the most common setup uses elevated sensors. A 3D LiDAR is usually placed on the roof or on a short mast, often together with GNSS and IMU, to avoid blind spots from the vehicle and to keep a clear view of the horizon. Forward-facing RGB or stereo cameras cover the front, while wide-angle cameras are placed around the vehicle for 360° awareness. Radars are added at the front, rear, and sides to work reliably in dust, rain, or fog. This type of setup is described in research datasets such as RELLIS-3D (Warthog) and

Table 3

Comparison of sensor parameters used in autonomous vehicles

Sensor	FOV	Range	Resolution / Rate	Accuracy	Data latency
OS2 LiDAR	360° H × ~22.5° V	400 m	—	±0.1 cm	< 10 ms
Ultra Puck VLP-32C	360° H × 40° V	200 m	—	±3 cm	100 ms
ZED X camera	110° H × 80° V × 120° D	≈**66.7 m**	~1200p, 60 fps	< 0.4% at 2 m, < 7% at 20 m	30 ms
FL-KTD-60 (TV)	180° H	≈**40.7 m**	1920×1080	—	30 ms
FL-KTD-60 (IR)	180° H	≈**13.6 m**	640×480	—	30 ms
SRR7 radar	~75° az	160 m	0.2 m range res.	±0.1 m/s	30 ms
AC1000T radar	~70° az	200 m	—	—	40 ms
TALIN 1000 IMU	—	—	—	5 mil heading accuracy	10 ms
IMU+	—	—	—	0.5°/h, 20 μg/h bias	5 ms
TFS20-L ToF	—	20 m	—	6 cm	4 ms

GOOSE (MuCAR-3), as well as in heavy off-road demonstrators like CMU Crusher and Oshkosh TerraMax. Radar surveys also recommend including SRR/MRR sensors to ensure perception under poor visibility [46, 63, 96–98].

A second common setup focuses on the near field and on detecting negative obstacles such as ditches or drop-offs. In this design, a short-range LiDAR is mounted low on the vehicle and tilted toward the ground. It is often combined with stereo or ToF cameras at the front bumper, so the ground is sampled more densely a few meters ahead of the vehicle. Studies show that the choice of sensor height and tilt can greatly reduce the "blind zone." For example, tilting a LiDAR by 40° reduced the blind area from about 3 m to only 0.21 m. This shows why low-mounted sensors are important, even when most sensors are placed high [42, 43].

A historical reference for high-speed driving in open terrain is the "desert-style" setup: several 2D laser scanners placed on the roof at different tilts, combined with a long-range camera and radars. This design was used by Stanley, the winner of the DARPA Grand Challenge, and demonstrated the benefits of high mounting and sensor redundancy. Modern off-road vehicles often use hybrid setups that combine the elevated configuration with low-mounted "anti-hole" sensors and perimeter radars, giving both global awareness and local safety [45].

The vehicle, in its current configuration as presented in Fig. 2a, is equipped with standard components that allow its operation and environmental perception. It includes power distribution units (PDU), an inertial measurement unit (IMU TALIN 3000), and a vehicle protection system (VPS) with the OBRA-3 self-defense system. In addition, the vehicle features a perimeter surveillance system (PSS) based on two KTD-90 modules and one KTD-60 module, which improves the situational awareness of the crew. The system also includes periscope cameras and a rearview camera for the driver. Cameras that are part of the PSS are managed by an image processing unit, which displays the video feed on the control computers and troop compartment consoles. The camera integrated into the periscope system has a separate image processing unit.

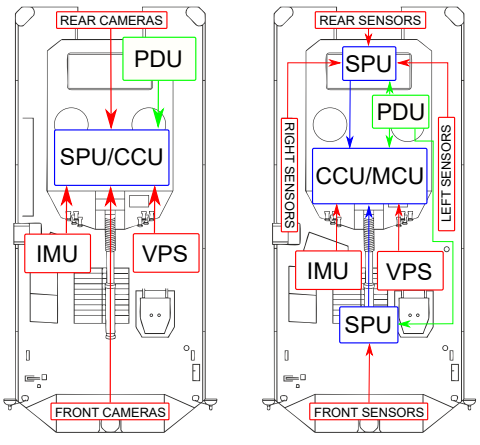

Fig. 2. Vehicle schematics: **a** existing systems, **b** proposed sensor architecture

The overall sensor architecture in the autonomous tracked vehicle, as depicted in Fig. 2b, is designed to enable 360-degree environmental perception. The sensor layout is divided into four main sectors: front, rear, left side, and right side. The front sensors are responsible for object detection in the direction of movement, allowing for early reactions to changing conditions and potential threats. Rear sensors assist with reverse maneuvers, which are critical for tasks such as backing up or parking in challenging terrain. Side sensors, placed on the left and right sides of the vehicle, support operations such as navigating through narrow spaces or executing turning maneuvers.

The sensors are integrated with processing units labeled in the diagram as SPU (sensor processing unit) and CCU/MCU (central control unit/master control unit). The SPU is responsible for local processing of data received from sensors in each sector, reducing the computational load on the central unit and enabling faster real-time decision-making. The CCU/MCU serves as the central data management hub, integrating information from all SPU units and coordinating the vehicle actuators and higher-level planning processes.

Two communication protocols have been adopted: CAN and Gigabit Ethernet TSN. The CAN standard ensures reliable communication between onboard controllers, propulsion systems, and low-bandwidth sensors such as ToF sensors. Ethernet TSN (time sensitive networking) enables deterministic high-bandwidth data transmission, which is essential for vision systems, LiDARs, and real-time data processing.

The autonomy system must be compatible with existing control, power, and communication subsystems. Additionally, it must precisely coordinate the operation of existing actuators to maintain full operational functionality. To achieve seamless integration, interface compatibility and redundancy of critical functions must be ensured.

In the sensor architecture of the autonomous tracked vehicle, four sensor configuration variants have been proposed (Fig. 3), incorporating LiDAR (OS2), stereoscopic cameras (ZED X), a module combining 3 daytime and IR cameras (FL-KTD-60), ToF sensors (TFS20-L), and radar (SRR7). Additionally, it has been assumed that measurements from the built-in IMU system of the TALIN 3000 series will be used for sensor fusion. Each variant offers unique characteristics in environmental perception. During sensor placement on the vehicle, local heat sources, such as exhaust or condenser, which could interfere with or distort readings, were taken into account. Below, a detailed characterization and analysis of the advantages and disadvantages of each variant are presented.

Variant 1: LiDAR OS2 and Daytime/IR Cameras (FL-KTD-60) presented in Fig. 3a

LiDAR OS2 (blue) positioned at the front of the vehicle enables obstacle detection and the creation of three-dimensional terrain maps. Daytime and IR cameras FL-KTD-60 (red) support navigation in low-visibility conditions.

Advantages:

- Precise 3D environmental perception thanks to LiDAR.
- Effective operation at night and in adverse weather conditions due to IR cameras.
- Rapid obstacle detection at short and medium distances.

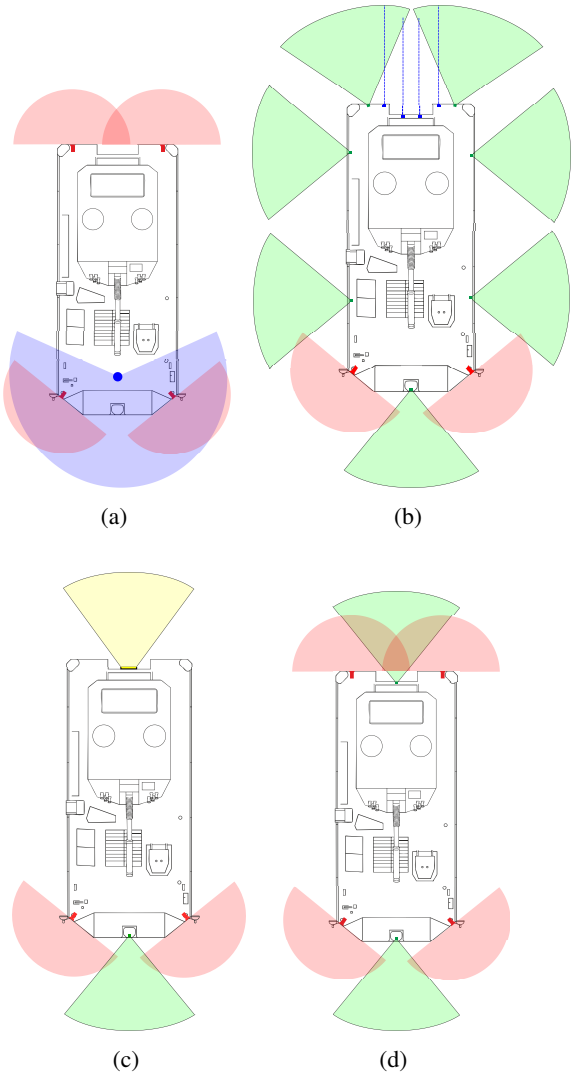

Fig. 3. Sensor placement variants: (a) variant 1, (b) variant 2, (c) variant 3, (d) variant 4

Disadvantages:

- Issues with detecting low-reflectivity objects for LiDAR.
- Vehicle may be easily detected due to the visible laser beam.
- Potential activation of the OBRA-3 self-defense system on the vehicle or an accompanying allied vehicle due to the LiDAR laser beam.
- Possible interference with IR cameras from external and internal heat sources, such as exhaust or condenser.
- Limited capability in monitoring lateral sectors.

Variant 2: Stereoscopic Cameras ZED X and ToF Sensors TFS20-L presented in Fig. 3b

Stereoscopic cameras ZED X (green) positioned around the vehicle provide 360° environmental perception. The TFS20-L (blue) ToF sensors placed in the rear enable distance measurements to obstacles during reversing.

Advantages:

- Full environmental perception due to camera placement around the vehicle.
- Precise distance measurements for maneuvering in confined spaces.
- Ability to analyze depth and terrain structure.

Disadvantages:

- Image quality issues from stereoscopic cameras in low-light conditions.
- Limited effectiveness of ToF sensors when dirty.
- High computational resource demand for SPU.

Variant 3: Radar SRR7 and Daytime/IR Cameras FL-KTD-60 presented in Fig. 3c

Radar SRR7 (yellow) mounted at the rear provides object detection in difficult conditions (mud from tracks) and is activated only during reversing. FL-KTD-60 cameras (red) monitor the area in front of the vehicle (primary sensors).

Advantages:

- Radar reliability in fog, rain, and snow conditions.
- IR cameras can operate at night without additional lighting.
- Low hardware requirements for SPU.

Disadvantages:

- Limited radar capability for precise object shape recognition.
- Lack of environmental information on the sides of the vehicle.
- Narrower radar field of view compared to LiDARs and stereoscopic cameras.

Variant 4: Daytime/IR Cameras FL-KTD-60 and Stereoscopic Cameras ZED X presented in Fig. 3d

FL-KTD-60 cameras (red) positioned at the vehicle corners provide wide-angle observation of the environment from the front and rear. Stereoscopic cameras (green) enable depth analysis and object tracking in blind spots.

Advantages:

- Full visual coverage of the vehicle front and rear zones.
- Increased safety due to passive sensor usage.
- Moderate hardware requirements for SPU.

Disadvantages:

- No coverage of the vehicle lateral zones.
- Lower terrain mapping accuracy.

Variant 1 represents a classic sensor layout on an autonomous vehicle, allowing for easy terrain mapping with an emphasis on forward driving. The use of LiDAR enhances the quality and accuracy of the generated map at the cost of increased computational load on the SPU. Additionally, side-mounted cameras could be added to eliminate blind spots during real-time observation. The FL-KTD-60 cameras enable both daytime and nighttime operation. However, the use of LiDAR carries significant negative consequences. The laser is easily detectable by adversaries and can be targeted. Furthermore, the OBRA-3 self-defense system, like its counterparts from other manufacturers, detects laser beams illuminating the vehicle. Despite reducing the LiDAR's field of operation from 360° to 270° to avoid illuminating the OBRA-3 system, laser beam reflections from the surroundings may still interfere with its function. If autonomous mortars move in formation or convoy, LiDARs could trigger self-defense systems on neighboring vehicles.

Variant 2 provides a 360° environmental view, ensuring full situational awareness at the cost of a high computational load on the SPU. The stereoscopic cameras allow for more accurate environmental mapping and object classification compared to FL-KTD-60 cameras, but they have limited effectiveness in adverse weather conditions. Two FL-KTD-60 cameras are installed at the front of the vehicle, enabling stereoscopic vision at night. Furthermore, TFS20-L sensors are placed in the rear, acting as downward-facing parking sensors that activate only during reverse. This configuration is intended to facilitate maneuvering in difficult weather conditions and at night. However, there is a risk that laser beam reflections from these sensors may be detected by adversaries or interfere with vehicle self-defense systems.

Variant 3 is a simplified version of Variant 2, in which ToF sensors are replaced with radar. This configuration imposes the lowest computational demands of all proposed variants. The radar is engaged solely during reverse maneuvers, complicating hostile detection efforts and removing the risk of inadvertently triggering OBRA-3 systems.

Variant 4 consists exclusively of passive sensors. The use of such sensors eliminates the risk that the vehicle is targeted by adversaries. The combination of FL-KTD-60 and ZED-X cameras at the front and rear enables safe navigation under various weather conditions and at night. The absence of side sensors reduces the computational load on the SPU while still allowing the vehicle to accomplish its designated tasks.

10. SENSOR TIMING AND RELIABLE FORWARD RECOGNITION RANGE

This section estimates reliable forward recognition range using a stopping model that includes sensor timing and assumed vehicle maximum speeds. The model is applied to the four sensing architectures in Fig. 3a–3d. Ranges and latencies come from Table 3 and from the timing needs defined earlier, namely synchronization, multi-rate sampling, VSLAM, and planning. The structure follows the standard perception-reaction plus braking approach used in active safety and vehicle dynamics [99, 100]. The achievable mean deceleration a is set by track-soil interaction and by the brake or retarder system [101, 102]. A paved-road target speed of 65 km/h and an off-road cap of 40 km/h are used.

10.1. Timing budget

The processing chain is mapped to the timing budget

$$\tau_{\text{tot}} = T_{\text{gate}} + \tau_{\text{sensor}} + \tau_{\text{align}} + \tau_{\text{features}} + \tau_{\text{vslam}} + \tau_{\text{plan}} + \tau_{\text{control}+\tau_{\text{net}}}. \quad (1)$$

Camera frame timing of 30–60 fps and forward-collision warning practice support T_{gate} and camera latency values [99]. Millisecond-level time synchronization τ_{align} is provided by IEEE 1588 PTP [103]. Automotive 77 GHz radar update periods of 30–50 ms are standard [104]. Table 4 summarizes representative values after literature review.

10.2. Vibration, exposure, and radar processing

At about 50 km/h, steel tracks excite the vehicle structure near 50 Hz and elastomer tracks near 70 Hz. The inertial unit sampling rate should avoid aliasing of these motions, therefore $f_s^{\text{IMU}} \geq 500$ Hz with matched anti-alias filters and accurate timestamps is recommended [100]. Camera exposure is limited by geometric blur and by vibration. Let $\text{GSD}(r)$ denote the ground sample distance at range r in metres per pixel. The exposure time satisfies

$$T_{\text{exp}} \leq \min\left(\frac{0.5\,\text{GSD}(r)}{v}, \frac{1}{10\,f_{\text{vib}}}\right), \quad (2)$$

where the first term limits translation smear to half a pixel using the pinhole relation between scene motion and pixel motion, and the second term limits the integration to one-tenth of the dominant vibration period to freeze the oscillation. The pixel-motion model and the definition of $\text{GSD}(r)$ follow [111]. Rotating LiDAR integrates motion over the scan, therefore IMU-aided deskew and tightly coupled LiDAR. Inertial odometry are required to remove distortion. For radar, constant false alarm rate (CFAR) detection adapts the threshold to the local clutter and noise level to keep a set false alarm probability, and Doppler–angle gates accept only returns whose radial velocity and bearing are consistent with the current track and with the platform kinematics,

Table 4
Timing budget used in calculations

Stage / item	Symbol	Max (ms)	Support
Decision loop, camera 30 fps	T_{gate}	33	ISO 15623 FCW practice [99]
Sensor data latency, forward	τ_{sensor}	40	Camera ~30–40 ms [99], radar ~40 ms, LiDAR < 10 ms
Time sync and alignment	τ_{align}	3	IEEE 1588 PTP [103]
Feature extraction (det./segm./trk)	τ_{features}	35-120	Real-time DNN on embedded GPU [105, 106]
Visual SLAM	τ_{vslam}	150	Image→state latency incl. keyframe optimization [107]
Local planning (DWA/Frenet/MPC-short)	τ_{plan}	15	Short-horizon planners [108, 109]
Control and actuation path	τ_{control}	150	Brake-by-wire and hydraulic response bands [34]
Networking and jitter	τ_{net}	5-20	TSN over GbE with bounded latency [110]

which reduces false associations from vegetation micro-Doppler while preserving true targets [104].

10.3. Effect of sensor count on timing

Let N_{cam} be the number of camera streams used in the decision loop and P_{eff} the effective GPU concurrency (number of streams processed truly in parallel). If one stream needs t_{feat} for feature extraction, a practical upper bound is

$$\tau_{\text{features}} \approx \left\lceil \frac{N_{\text{cam}}}{P_{\text{eff}}} \right\rceil t_{\text{feat}} + t_{\text{sched}}, \tag{3}$$

where t_{sched} is a small scheduling overhead. Network delay grows with utilization $U = \sum_i \text{bitrate}_i / \text{link\_rate}$, so the worst-case increases from serialization and queuing,

$$\tau_{\text{net}} \approx \tau_{\text{net,base}} + \tau_{\text{queue}}(U). \tag{4}$$

Under hard synchronization, the decision cycle waits until all selected front, side, and rear streams are available. The feature stage must therefore process a batch of N_{cam} camera streams each cycle. The effective GPU parallelism is denoted P_{eff} and the per-stream feature time is t_{feat}. A small scheduling overhead t_{sched} covers kernel launch and buffering. For the heaviest variant an extra preprocessing allowance δ_{pre} is added for rectification and frame alignment. The model used is

$$\tau_{\text{features}} = \left\lceil \frac{N_{\text{cam}}}{P_{\text{eff}}} \right\rceil t_{\text{feat}} + t_{\text{sched}} + \delta_{\text{pre}}, \tag{5}$$

where the variables values are assumed to be equal $P_{\text{eff}} = 2$, $t_{\text{feat}} = 25$ ms, $t_{\text{sched}} = 5$ ms, $\delta_{\text{pre}} = 5$ ms for variant 4 and 0 for other variants.

Network time includes a base switching and timestamping budget plus an increment that grows with the number of synchronized streams and added modalities:

$$\tau_{\text{net}} = \tau_{\text{net,base}} + \Delta_{\text{net}}, \qquad \tau_{\text{net,base}} = 5 \text{ ms}. \tag{6}$$

The increment Δ_{net} is set per variant to reflect fan-in and scheduled traffic.

AoI (Age of Information) is taken as one full update period of the slowest synchronized *non-camera* modality in the loop for LiDAR at 20 Hz $\Delta_{\text{AoI}} = 50$ ms, radar at 33 Hz, $\Delta_{\text{AoI}} = 30$ ms, ToF at 30 fps, $\Delta_{\text{AoI}} = 33$ ms. The common worst-case baseline for all variants, excluding τ_{features}, τ_{net}, and Δ_{AoI}, is

$$T_{\text{gate}}(33) + \tau_{\text{sensor}}(40) + \tau_{\text{align}}(3) + \tau_{\text{vslam}}(150) + \tau_{\text{plan}}(15) + \tau_{\text{control}}(150) = 391 \text{ ms}. \tag{7}$$

Totals reported in Table 5 equal

$$\tau_{\text{tot,max}} + \Delta_{\text{AoI}} = 391 + \tau_{\text{features}} + \tau_{\text{net}} + \Delta_{\text{AoI}}. \tag{8}$$

Table 5 summarizes the four sensing configurations, variants 1–4. The off-road operating speed is limited at 40 km/h.

Table 5
Sensor architectures under hard synchronization: synchronized set, stream count, and worst–case timing (ms)

Variant	N_{cam}	τ_{features}	τ_{net}	Δ_{AoI}	Total $\tau_{\text{tot,max}}+\Delta_{\text{AoI}}$
1	4	55	8	50 (LiDAR 20 Hz)	**504**
2	8	105	12	33 (ToF 30 fps)	**541**
3	4	55	8	30 (radar 33 Hz)	**484**
4	6	85	10	0 (camera-gated)	**486**

10.4. Stopping condition with sensor timing

Let v be the speed when a hazard first becomes detectable and let the end-to-end timing consist of the worst-case processing delay plus the AoI of the slow fused modality. A sufficient condition to stop before the obstacle is

$$R_{\text{min}} \geq v\left(\tau_{\text{tot,max}} + \Delta_{\text{AoI}}\right) + \frac{v^2}{2a} + s_{\text{margin}}, \tag{9}$$

where R_{min} is the reliable forward recognition range, a is the mean achievable deceleration, and s_{margin}=10 m. The calculations below use hard-sync totals $\tau_{\text{tot,max}}+\Delta_{\text{AoI}}$ with $a \in \{2.0, 3.0\}$ m/s^2 and design speeds 65 km/h and 40 km/h. The calculated R_{min} are shown in Table 6.

10.5. Variant assessment against minimum criteria

The four sensing variants are assessed against the consolidated criteria.

Clear-weather forward recognition ranges are 400 m for variant 1 (OS2 LiDAR with two FL–KTD–60) and about 67 m for variants 2–4 (two FL–KTD–60 plus one ZED X in front, computed for a 1.0 m target at 15 px). With the totals in Table 6, the 65 km/h stopping requirement is $R_{\text{min}} \approx 100$ m for a=2.0 and $R_{\text{min}} \approx 74$ m for a=3.0. Therefore, only variant 1 satisfies all minima with margin, at the cost of managing laser emissions. Variants 2–4 are adequate for 40 km/h and offer wide FOV and good coverage, but their ~67 m forward horizon is too low at 65 km/h. To meet the criteria without lowering the road-speed target, these camera-centric variants should add a forward long-range modality (radar or LiDAR), in low light enviroment the IR reach is insufficient even for 30 km/h. The variants evaluated against the criteria are shown in Table 7.

If the ZED X stereo is removed and the forward arc uses only FL–KTD–60, the daylight TV channel yields a recognition horizon of ~ 40.7 m (1.0 m at 15 px) and the IR channel ~ 13.6 m. This cannot meet the 65 km/h requirement for any a considered, at 40 km/h it meets the requirement only in daylight with higher deceleration ($a \approx 3.0$ m/s^2).

The four sensor variants can be combined to form configurations tailored to specific missions and threat conditions. In our assessment, the variants presented are the most practical for a tracked platform. Among them, variant 4 offers a balanced trade-off between situational awareness (360° coverage with overlapping fields of view) and processing load on the SPU. When passive mode is required, excluding LiDAR, ToF, and

Table 6

Reliable forward recognition range $R^*_{\min}$ from $R_{\min} \geq v(\tau_{\text{tot,max}}+\Delta_{\text{AoI}}) + \frac{v^2}{2a} + s_{\text{margin}}$ with s_{margin}=10 m

Variant	Total time (ms)	$R^*_{\min}$ @ 65 km/h, a=2.0	$R^*_{\min}$ @ 65 km/h, a=3.0	$R^*_{\min}$ @ 40 km/h, a=2.0	$R^*_{\min}$ @ 40 km/h, a=3.0
1	504	100.60 m	73.43 m	46.46 m	36.18 m
2	541	101.27 m	74.10 m	46.88 m	36.59 m
3	484	100.24 m	73.07 m	46.24 m	35.95 m
4	486	100.28 m	73.11 m	46.26 m	35.98 m

Table 7

Variants vs. minimum criteria (**+** meets, **a** conditional/marginal, – fails). Time processing without time of braking $\tau_{\text{control}} \approx 140$

Var.	Stop at 65 (a=2/3)	Stop at 40 (a=2/3)	Time (< 350 ms)	FOV (≥ 120°×60°)	Accuracy (min specs)	Low-vis (forward arc)	Coverage (no forward occl.)	Signature
1	+/+	+/+	-	+	+	+	+	**a** (laser)
2	–/**a***	+/+	-	+	+	**a**†	+	+
3	–/**a***	+/+	+	+	+	**a**†	+	+
4	–/**a***	+/+	+‡	+	+	**a**†	+	+

* Meets 65 km/h only in the optimistic case (a=3.0 m/s^2) and clear visibility; the ~67 m horizon is marginal vs. ~67 m required.

† Camera-centric forward sensing is not robust to fog/dust/rain/night; add forward radar or LiDAR (or reduce speed) to guarantee $R_{\min} \geq 50$ m.

‡ Larger camera set: necessary parallel feature extraction and hard-sync to slow modalities.

radar reduces detectability of the vehicle and crew. Under such conditions the self-propelled mortar tasks can be executed at the design speeds (≈ 65 km/h on paved roads, capped at ≈ 40 km/h off-road) in clear weather.

However, in degraded visibility (night without skyglow, fog, dust, rain, or snow), passive-only sensing shortens reliable recognition range and tightens the stopping constraint, which can force speed reductions and shrink maneuver margins. For those conditions, we recommend a contingent/switchable configuration that adds a low-signature forward radar or long-range LiDAR (enabled only when EMCON constraints allow) to preserve detection range and maintain the required safety margins.

11. DISCUSSION

In the analysis of the presented variants, the key challenge is finding a balance between the quality of environmental perception and the computational load on the system. Variants utilizing active sensors, such as LiDAR or ToF, enable more precise terrain mapping but simultaneously increase the risk of vehicle detection by adversaries and impose significant computational demands on the SPU. On the other hand, the exclusive use of passive sensors limits situational awareness in adverse weather conditions but enhances overall security. The choice of a specific sensor configuration should be based on the nature of the mission in which the vehicle will operate.

An additional challenge is the coordination of vehicles operating in formation, particularly the impact of active sensors on self-defense and detection systems, targeting systems, and observation equipment. Possible interference with neighboring vehicles caused by active sensors could lead to unintended activations of defensive systems, crew blinding, false alarms, and, consequently, tactical misjudgments that hinder operational effectiveness.

The proposed sensor architecture has been tailored to the operational environment and combat conditions in which the vehicle will function. The analysis carried out in this article indicates that the selected sensors provide adequate terrain perception, considering variable weather conditions and potential disturbances. Variants incorporating FL-KTD-60 and ZED-X cameras ensure operational capability during both day and night, while the integration of LiDAR enhances maneuvering efficiency in challenging terrain. A crucial aspect remains selecting the appropriate configuration for a specific mission to maintain an optimal balance between situational awareness and vehicle and crew safety.

12. CONCLUSIONS

The analysis of the sensor architecture for the autonomous tracked vehicle has demonstrated that the proper selection and placement of sensors are critical for its operational capabilities in combat environments. The use of LiDARs, FL-KTD-60 vision cameras, ToF sensors, radars, and IMU units enables effective terrain mapping and real-time object detection. The considered sensor configurations differ in terms of situational awareness, computational requirements, and susceptibility to enemy detection. Particular attention has been given to the trade-off between enhanced environmental perception and minimizing detection risk, which is crucial in military applications.

Sensor data fusion plays a key role in ensuring system reliability and improving vehicle perception accuracy. Integrating data from cameras, LiDARs, radars, and inertial measurement units helps reduce errors stemming from individual sensor limitations while increasing resistance to interference and adverse environmental conditions. The application of SLAM algorithms and multisensor analysis methods enhances the synchronization of terrain information, improving navigation and autonomous route planning. A well-designed sensor architecture, supported by advanced data fusion algorithms, enhances the accuracy of environmental mapping and decision-making reliability in combat conditions.

REFERENCES

[1] "Taxonomy and definitions for terms related to driving automation systems for on-road motor vehicles," SAE International, Tech. Rep. SAE J3016, 2021.

[2] A.N. Ouda and A. Mohamed, "Autonomous fuzzy heading control for a multi-wheeled combat vehicle," *Int. J. Robot. Control Syst.*, vol. 1, no. 1, pp. 90–101, 2021, doi: 10.31763/ijrcs.v1i1.286.

[3] S. Nahavandi *et al.*, "Autonomous convoying: A survey on current research and development," *IEEE Access*, vol. 10, pp. 13 663–13 683, 2022, doi: 10.1109/ACCESS.2022.3147251.

[4] K.D. Ahmadi, A.J. Rashidi, and A.M. Moghri, "Design and simulation of autonomous military vehicle control system based on machine vision and ensemble movement approach," *J. Supercomput.*, vol. 78, no. 15, pp. 17 309–17 347, 2022, doi: 10.1007/s11227-022-04565-6.

[5] N. Wang, X. Li, K. Zhang, J. Wang, and D. Xie, "A survey on path planning for autonomous ground vehicles in unstructured environments," *Machines*, vol. 12, no. 1, p. 31, 2024, doi: 10.3390/machines12010031.

[6] I. Bae and J. Hong, "Survey on the developments of unmanned marine vehicles: Intelligence and cooperation," *Sensors*, vol. 23, p. 4643, 2023, doi: 10.3390/s23104643.

[7] F. Rovira-Más, "Sensor architecture and task classification for agricultural vehicles and environments," *Sensors*, vol. 10, pp. 11 226–11 247, 2010, doi: 10.3390/s101211226.

[8] X. Wang, K. Li, and A. Chehri, "Multi-sensor fusion technology for 3d object detection in autonomous driving: A review," *IEEE Trans. Intell. Transp. Syst.*, vol. 25, no. 2, pp. 1148–1165, 2023, doi: 10.1109/TITS.2023.3317372.

[9] D.J. Yeong, G. Velasco-Hernandez, J. Barry, and J. Walsh, "Sensor and sensor fusion technology in autonomous vehicles: A review," *Sensors*, vol. 21, p. 2140, 2021, doi: 10.3390/s21062140.

[10] Y. Boersma, "Robust localization and navigation for autonomous, military robots in gnss-denied environments," Master's thesis, University of Twente, 2022.

[11] O.Y. Al-Jarrah, A.S. Shatnawi, M.M. Shurman, O.A. Ramadan, and S. Muhaidat, "Exploring deep learning-based visual localization techniques for uavs in gps-denied environments," *IEEE Access*, vol. 12, pp. 113 049–113 071, 2024, doi: 10.1109/ACCESS.2024.3440064.

[12] E. Blasch *et al.*, "Machine learning/artificial intelligence for sensor data fusion–opportunities and challenges," *IEEE Aerosp. Electron. Syst. Mag.*, vol. 36, no. 7, pp. 80–93, 2021, doi: 10.1109/MAES.2020.3049030.

[13] B. Shahian Jahromi, T. Tulabandhula, and S. Cetin, "Real-time hybrid multi-sensor fusion framework for perception in autonomous vehicles," *Sensors*, vol. 19, p. 4357, 2019, doi: 10.3390/s19204357.

[14] L. Elkins, D. Sellers, and W.R. Monach, "The autonomous maritime navigation (amn) project: Field tests, autonomous and cooperative behaviors, data fusion, sensors, and vehicles," *J. Field Robot.*, vol. 27, no. 6, pp. 790–818, 2010, doi: 10.1002/rob.20367.

[15] W. Liu, Y. Liu, and R. Bucknall, "Filtering based multi-sensor data fusion algorithm for a reliable unmanned surface vehicle navigation," *J. Mar. Eng. Technol.*, vol. 22, no. 2, pp. 67–83, 2023, doi: 10.1080/20464177.2022.2031558.

[16] J. Fayyad, M.A. Jaradat, D. Gruyer, and H. Najjaran, "Deep learning sensor fusion for autonomous vehicle perception and localization: A review," *Sensors*, vol. 20, p. 4220, 2020, doi: 10.3390/s20154220.

[17] M.H. Harun, S.S. Abdullah, M.S.M. Aras, and M.B. Bahar, "Sensor fusion technology for unmanned autonomous vehicles (uav): A review of methods and applications," in *Proc. 2022 IEEE 9th International Conference on Underwater System Technology: Theory and Applications (USYS)*, Kuala Lumpur, Malaysia, 2022, pp. 1–8, doi: 10.1109/USYS56283.2022.10072667.

[18] J. Yang, S. Liu, H. Su, and Y. Tian, "Driving assistance system based on data fusion of multisource sensors for autonomous unmanned ground vehicles," *Comput. Netw.*, vol. 192, p. 108053, 2021, doi: 10.1016/j.comnet.2021.108053.

[19] D. Parekh *et al.*, "A review on autonomous vehicles: Progress, methods and challenges," *Electronics*, vol. 11, p. 2162, 2022, doi: 10.3390/electronics11142162.

[20] J.J. Galán, R.A. Carrasco, and A. LaTorre, "Military applications of machine learning: A bibliometric perspective," *Mathematics*, vol. 10, p. 1397, 2022, doi: 10.3390/math10091397.

[21] M. Bistron and Z. Piotrowski, "Artificial intelligence applications in military systems and their influence on sense of security of citizens," *Electronics*, vol. 10, p. 871, 2021, doi: 10.3390/electronics10070871.

[22] W. Wang, H. Liu, W. Lin, Y. Chen, and J.A. Yang, "Investigation on works and military applications of artificial intelligence," *IEEE Access*, vol. 8, pp. 131 614–131 625, 2020, doi: 10.1109/ACCESS.2020.3009840.

[23] D.J. Yeong, J. Barry, and J. Walsh, "A review of multi-sensor fusion system for large heavy vehicles off road in industrial environments," in *Proc. 2020 31st Irish Signals and Systems Conference (ISSC)*, Letterkenny, Ireland, 2020, pp. Letterkenny, Ireland, 11–12 June 2020, doi: 10.1109/ISSC49989.2020.9180186.

[24] Z. Wang, Y. Wu, and Q. Niu, "Multi-sensor fusion in automated driving: A survey," *IEEE Access*, vol. 8, pp. 2847–2868, 2019, doi: 10.1109/ACCESS.2019.2962554.

[25] S. Symes, E. Blanco-Davis, T. Graham, J. Wang, and E. Shaw, "Cyberattacks on the maritime sector: A literature review," *J. Mar. Sci. Appl.*, vol. 23, no. 4, pp. 689–706, 2024, doi: 10.1007/s11804-024-00443-0.

[26] M. Oreyomi and H. Jahankhani, "Challenges and opportunities of autonomous cyber defence (acyd) against cyber-attacks," in *Blockchain and Other Emerging Technologies for Digital Business Strategies*, 2022, pp. 239–269, doi: 10.1007/978-3-030-98225-6_9.

[27] P. Théron and A. Kott, "When autonomous intelligent goodware will fight autonomous intelligent malware: A possible future of

cyber defense," in *MILCOM 2019 IEEE Military Communications Conference (MILCOM)*, Norfolk, VA, USA, 2019, pp. 1–7, doi: 10.1109/MILCOM47813.2019.9021038.

[28] M. Pitale, A. Abbaspour, and D. Upadhyay, "Inherent diverse redundant safety mechanisms for ai-based software elements in automotive applications," arXiv preprint arXiv:2402.08208, 2024, doi: 10.48550/arXiv.2402.08208.

[29] "Aectp-250: Electrical and electromagnetic environmental conditions (edition 1)," NATO Standardization Agency, Tech. Rep., 2009, copy available in HSW S.A. archive, [Accessed on 24 January 2025].

[30] "No-a-stanag-4370/aectp-300-16:2022 — sprzęt wojskowy – klimatyczne badania środowiskowe (metoda 300 i kolejne)," Inspektorat Wsparcia Sił Zbrojnych / MON (Polska Norma Obronny, NO-A), Tech. Rep., 2022, copy available in HSW S.A. archive, [Accessed on 24 January 2025].

[31] "Mil-std-883: Test method standard — microcircuits," U.S. Department of Defense, Tech. Rep., 2021, copy available in HSW S.A. archive, [Accessed on 24 January 2025].

[32] "Mil-std-810h: Environmental engineering considerations and laboratory tests," U.S. Department of Defense, Tech. Rep., 2019, copy available in HSW S.A. archive, [Accessed on 24 January 2025].

[33] A. Kiński, "Borsuki rosną w stalowej woli," *Wojsko i Technika*, vol. 9, pp. 22–26, 2022, (in Polish).

[34] HSW S.A., "Bwp borsuk datasheet," 2025, available in HSW S.A. archive, [Accessed on 17 January 2025].

[35] Wikipedia contributors, "M120 rak," [Online]. Available: https://pl.wikipedia.org/wiki/M120_Rak, 2024, [Accessed: 17 February 2025].

[36] "Tc 3-22.69: Advanced situational awareness," Headquarters, Department of the Army, Tech. Rep., April 2021, copy available in HSW S.A. archive, [Accessed on 24 January 2025].

[37] "Atp 3-09.42: Fire support for the brigade combat team," Headquarters, Department of the Army, Tech. Rep., March 2016, copy available in HSW S.A. archive, [Accessed on 24 January 2025].

[38] K. Katona, H.A. Neamah, and P. Korondi, "Obstacle avoidance and path planning methods for autonomous navigation of mobile robot," *Sensors*, vol. 24, no. 11, p. 3573, 2024, doi: 10.3390/s24113573.

[39] D. Scaramuzza and F. Fraundorfer, "Visual odometry [tutorial]," *IEEE Robot. Autom. Mag.*, vol. 18, no. 4, pp. 80–92, 2011, doi: 10.1109/MRA.2011.943233.

[40] J.A. Hesch, D.G. Kottas, S.L. Bowman, and S.I. Roumeliotis, "Consistency analysis and improvement of vision-aided inertial navigation," *Int. J. Robot. Res.*, vol. 33, no. 1, pp. 182–201, 2014, doi: 10.1177/0278364913509675.

[41] D.J. Fagnant and K. Kockelman, "Preparing a nation for autonomous vehicles: Opportunities, barriers and policy recommendations," *Transp. Res. Part A Policy Pract.*, vol. 77, pp. 167–181, 2015, doi: 10.1016/j.tra.2015.04.003.

[42] C. Goodin, J. Carrillo, J.G. Monroe, D.W. Carruth, and C.R. Hudson, "An analytic model for negative obstacle detection with lidar and numerical validation using physics-based simulation," *Sensors*, vol. 21, no. 9, p. 3211, 2021, doi: 10.3390/s21093211.

[43] P. Xie *et al.*, "Lidar-based negative obstacle detection for unmanned ground vehicles in orchards," *Sensors*, vol. 24, no. 24, p. 7929, 2024, doi: 10.3390/s24247929.

[44] H. Koyasu, Y. Uno, K. Iizuka, Y. Nishi, and E. Koyanagi, "Slip-compensated odometry for tracked vehicle on loose and weak slope," *ROBOMECH J.*, vol. 4, no. 1, p. 7, 2017, doi: 10.1186/s40648-017-0095-1.

[45] S. Thrun, "Stanley: The robot that won the darpa grand challenge," *J. Field Robot.*, vol. 23, no. 9, pp. 661–692, 2006, doi: 10.1002/rob.20147.

[46] A. Broggi *et al.*, "The passive sensing suite of the terramax autonomous vehicle," in *2008 IEEE Intelligent Vehicles Symposium*, Eindhoven, The Netherlands, 2008, pp. 769–774, doi: 10.1109/IVS.2008.4621208.

[47] Bumar PCO, "Ssp-1 "obra-3" datasheet," 2014, available in Bumar PCO archive, [Accessed on 17 November 2014].

[48] Y. Li and J. Ibanez-Guzman, "Lidar for autonomous driving: The principles, challenges, and trends for automotive lidar and perception systems," arXiv preprint arXiv:2004.08467, 2020, doi: 10.1109/MSP.2020.2973615.

[49] R. Frehlich, "Comparison of 2-and 10-µm coherent doppler lidar performance," *J. Atmos. Oceanic Technol.*, vol. 12, no. 2, pp. 415–420, 1995, doi: 10.1175/1520-0426(1995)012<0415:COACDL>2.0.CO;2.

[50] World Bank Group, "The climate knowledge portal," [Online]. Available: https://climateknowledgeportal.worldbank.org/, 2025, [Accessed: 23 January 2025].

[51] Copernicus Program, "Copernicus climate change service," [Online]. Available: https://cds.climate.copernicus.eu/, 2025, [Accessed: 23 January 2025].

[52] I. Anders, "Climate change in central and eastern europe," in *Managing Protected Areas in Central and Eastern Europe under Climate Change*, 2014, pp. 17–30, doi: 10.1007/978-94-007-7960-0_2.

[53] K. Blazejczyk, "Natural and human environment of poland," in *A Geographical Overview: Climate and Bioclimate of Poland*, 2006.

[54] Z. Kundzewicz and P. Matczak, "Climate change regional review: Poland," *Wiley Interdiscip. Rev. Clim. Change*, vol. 3, pp. 297–311, 2012, doi: 10.1002/wcc.175.

[55] A. Teit, *Atlas of the World*, 2nd ed. Washington, DC: National Geographic Society, 2019.

[56] "Stanag 4370 / aectp-200: Environmental conditions for defence materiel," NATO Standardization Office, Tech. Rep., 2009, copy available in HSW S.A. archive, [Accessed on 24 January 2025].

[57] "Aectp-300: Climatic environmental tests," NATO Standardization Office, Tech. Rep., 2006, copy available in HSW S.A. archive, [Accessed on 24 January 2025].

[58] *IEC 60529: Degrees of Protection Provided by Enclosures (IP Code)*, International Electrotechnical Commission / NEMA (US Adoption) Std., 2020, copy available in HSW S.A. archive, [Accessed on 24 January 2025].

[59] "Top 2-2-612: Fording (wheeled and tracked vehicles)," U.S. Army Test and Evaluation Command, Tech. Rep., 2007, copy available in HSW S.A. archive, [Accessed on 24 January 2025].

[60] *CIE S 011/E:2003 Spatial Distribution of Daylight — CIE Standard General Sky*, [Online]. Available: https://cie.co.at/publications/spatial-distribution-daylight-cie-standard-general-sky, International Commission on Illumination (CIE) Std., 2003, [Accessed on 24 January 2025].

[61] R. Perez, R. Seals, and J. Michalsky, "All-weather model for sky luminance distribution — preliminary configuration and validation," *Solar Energy*, vol. 50, no. 3, pp. 235–245, 1993, doi: 10.1016/0038-092X(93)90017-I.

[62] "Aectp-230: Climatic conditions (aectp-200 category 230 leaflets)," NATO Standardization Office, Tech. Rep., 2009, copy available in HSW S.A. archive, [Accessed on 24 January 2025].

[63] A. Stentz, J. Bares, T. Pilarski, and D. Stager, "The crusher system for autonomous navigation," in *AUVSI's Unmanned Systems North America*, 2007.

[64] SICK AG, "Lms 291 laser measurement system — product datasheet," [Online]. Available: https://sicktoolbox.sourceforge.net/docs/sick-lms-technical-description.pdf, 2004, [Accessed on 24 January 2025].

[65] L. Matthies *et al.*, "Obstacle detection in foliage with ladar and radar," in *Robotics Research*, ser. Springer Tracts in Advanced Robotics. Springer, 2005, vol. 15, pp. 291–302, doi: 10.1007/11008941_31.

[66] T. Overbye and S. Saripalli, "Radar-only off-road local navigation," in *Proc. IEEE Intelligent Transportation Systems Conference (ITSC)*, 2023, doi: 10.48550/arXiv.2310.17620.

[67] N.B.F. da Silva, D.B. Wilson, and K.R.L.J. Branco, "Performance evaluation of the extended kalman filter and unscented kalman filter," in *2015 International Conference on Unmanned Aircraft Systems (ICUAS)*, Denver, CO, USA, 2015, pp. 733–741, doi: 10.1109/ICUAS.2015.7152356.

[68] K. Marino, R. Salakhutdinov, and A. Gupta, "The more you know: Using knowledge graphs for image classification," arXiv preprint arXiv:1612.04844, 2016, doi: 10.48550/arXiv.1612.04844.

[69] M.S. Arulampalam, S. Maskell, N. Gordon, and T. Clapp, "A tutorial on particle filters for online nonlinear/non-gaussian bayesian tracking," *IEEE Trans. Signal Process.*, vol. 50, no. 2, pp. 174–188, 2002, doi: 10.1109/78.978374.

[70] L. Mutauranwa and M. Nleya, "An efficient median filter in a robot sensor soft ip-core," in *2013 Africon*, Pointe aux Piments, Mauritius, 2013, pp. 1–5, doi: 10.1109/AFRCON.2013.6757651.

[71] B. Suwandi, T. Kitasuka, and M. Aritsugi, "Vehicle vibration error compensation on imu-accelerometer sensor using adaptive filter and low-pass filter approaches," *J. Inf. Process.*, vol. 27, pp. 33–40, 2019, doi: 10.2197/ipsjjip.27.33.

[72] M. Abu Bakr and S. Lee, "Distributed multisensor data fusion under unknown correlation and data inconsistency," *Sensors*, vol. 17, no. 11, p. 2472, 2017, doi: 10.3390/s17112472.

[73] V. De Silva, J. Roche, and A. Kondoz, "Robust fusion of lidar and wide-angle camera data for autonomous mobile robots," *Sensors*, vol. 18, no. 8, p. 2730, 2018, doi: 10.3390/s18082730.

[74] T. Palpanas, D. Papadopoulos, V. Kalogeraki, and D. Gunopulos, "Distributed deviation detection in sensor networks," *ACM SIGMOD Rec.*, vol. 32, no. 4, pp. 77–82, 2003, doi: 10.1145/959060.959074.

[75] B. Baheti *et al.*, "Semantic scene segmentation in unstructured environment with modified deeplabv3+," *Pattern Recognit. Lett.*, vol. 138, pp. 223–229, 2020, doi: 10.1016/j.patrec.2020.07.029.

[76] A.O. Frâncani and M.R.O. Maximo, "Transformer-based model for monocular visual odometry: A video understanding approach," *IEEE Access*, 2025, doi: 10.48550/arXiv.2305.06121.

[77] D. Kumar and N. Muhammad, "Object detection in adverse weather for autonomous driving through data merging and yolov8," *Sensors*, vol. 23, p. 8471, 2023, doi: 10.3390/s23208471.

[78] C. Zhao *et al.*, "Monovit: Self-supervised monocular depth estimation with a vision transformer," in *Proc. 2022 International Conference on 3D Vision (3DV)*, Prague, Czech Republic, 2022, pp. 668–678, doi: 10.1109/3DV57658.2022.00077.

[79] G. Grisetti *et al.*, "A tutorial on graph-based slam," *IEEE Intell. Transp. Syst. Mag.*, vol. 2, pp. 31–43, 2010, doi: 10.1109/MITS.2010.939925.

[80] K. Berntorp, T. Hoang, and S. Di Cairano, "Motion planning of autonomous road vehicles by particle filtering," *IEEE Trans. Intell. Veh.*, vol. 4, pp. 197–210, 2019, doi: 10.1109/TIV.2019.2904394.

[81] Q. Liu *et al.*, "Global path planning for autonomous vehicles in off-road environment via an a-star algorithm," *Int. J. Veh. Auton. Syst.*, vol. 13, pp. 330–339, 2017, doi: 10.1504/IJVAS.2017.087148.

[82] A. Loganathan and N.S. Ahmad, "A systematic review on recent advances in autonomous mobile robot navigation," *Eng. Sci. Technol. Int. J.*, vol. 40, p. 101343, 2023, doi: 10.1016/j.jestch.2023.101343.

[83] E.J. Molinos, A. Llamazares, and M. Ocaña, "Dynamic window based approaches for avoiding obstacles in moving," *Robot. Auton. Syst.*, vol. 118, pp. 112–130, 2019, doi: 10.1016/j.robot.2019.05.003.

[84] Z. Zhao *et al.*, "Kinematics-aware model predictive control for autonomous high-speed tracked vehicles under off-road conditions," *Mech. Syst. Signal Process.*, vol. 123, pp. 333–350, 2019, doi: 10.1016/j.ymssp.2019.01.005.

[85] X. Wang *et al.*, "Deep reinforcement learning-based off-road path planning via low-dimensional simulation," *IEEE Trans. Intell. Veh.*, 2023, doi: 10.1109/TIV.2023.3347531.

[86] J. Schulte-Tigges, M. Förster, G. Nikolovski *et al.*, "Benchmarking of various lidar sensors for use in self-driving vehicles in real-world environments," *Sensors*, vol. 22, p. 7146, 2022, doi: 10.3390/s22197146.

[87] Ouster Inc., "Os2 lidar sensor," [Online]. Available: https://ouster.com/products/hardware/os2-lidar-sensor, 2024, [Accessed: 17 February 2025].

[88] Mapix Technologies, "Lidar scanner sensors," [Online]. Available: https://www.mapix.com/lidar-scanner-sensors/velodyne/, 2024, [Accessed: 17 February 2025].

[89] Stereolabs, "Zed x camera," [Online]. Available: https://www.stereolabs.com/en-pl/products/zed-x, 2024, [Accessed: 17 February 2025].

[90] Etronika, "Ktd-60 camera," [Online]. Available: https://www.etronika.pl/products/cameras/ktd-60/, 2024, [Accessed: 17 February 2025].

[91] Aptiv, "Gen7 radar family," [Online]. Available: https://www.aptiv.com/en/gen7-radar-family, 2024, [Accessed: 17 February 2025].

[92] ZF Group, "Cv sensor solutions," [Online]. Available: https://www.zf.com/products/en/cv/products_76432.html, 2024, [Accessed: 17 February 2025].

[93] Honeywell Aerospace, "Talin inertial land navigator family," [Online]. Available: https://aerospace.honeywell.com/us/en/products-and-services/product/hardware-and-systems/sensors/talin- inertial-land-navigator-family, 2024, [Accessed: 17 February 2025].

[94] Anello Photonics, "Imu plus," [Online]. Available: https://www.anellophotonics.com/products/imu-plus, 2024, [Accessed: 17 February 2025].

[95] Benewake, "Tfs20l sensor," [Online]. Available: https://en.benewake.com/TFS20L/index.html, 2024, [Accessed: 17 February 2025].

[96] P. Jiang, P. Osteen, M. Wigness, and S. Saripalli, "Rellis-3d dataset: Data, benchmarks and analysis," in *Proc. IEEE International Conference on Robotics and Automation (ICRA)*, vol. 2021, 2021, pp. 1110–1116, doi: 10.1109/ICRA48506.2021.9561251.

[97] P. Mortimer, R. Hagmanns, M. Granero, T. Luettel, J. Petereit, and H.-J. Wuensche, "The goose dataset for perception in unstructured environments," in *Proc. IEEE International Conference on Robotics and Automation (ICRA)*, Yokohama, Japan, 2024, doi: 10.1109/ICRA57147.2024.10611298.

[98] K. Harlow, H. Jang, T.D. Barfoot, A. Kim, and C. Heckman, "A new wave in robotics: Survey on recent mmwave radar applications in robotics," *IEEE Trans. Robot.*, vol. 40, pp. 4544–4560, 2024, doi: 10.1109/TRO.2024.3463504.

[99] *ISO 15623:2013 — Intelligent transport systems — Forward vehicle collision warning systems — Performance requirements and test procedures*, [Online]. Available: https://www.iso.org/standard/59244.html, International Organization for Standardization Std., 2013, [Accessed on 21 August 2025].

[100] R. Rajamani, *Vehicle Dynamics and Control*, 2nd ed. Springer, 2012, doi: 10.1007/978-1-4614-1433-9.

[101] J.Y. Wong, *Terramechanics and Off-Road Vehicle Engineering*, 2nd ed. Butterworth–Heinemann, 2010, doi: 10.1016/C2009-0-00403-6.

[102] J.Y. Wong, *Theory of Ground Vehicles*, 5th ed. Wiley, 2019, doi: 10.1002/9781119719984.

[103] *IEEE Std 1588-2008 — Precision Clock Synchronization Protocol for Networked Measurement and Control Systems*, IEEE Std., 2008, doi: 10.1109/IEEESTD.2008.4579760.

[104] M.A. Richards, *Fundamentals of Radar Signal Processing*, 2nd ed. McGraw–Hill, 2014.

[105] A. Bochkovskiy, C.-Y. Wang, and H.-Y.M. Liao, "Yolov4: Optimal speed and accuracy of object detection," *arXiv preprint*, 2020, doi: 10.48550/arXiv.2004.10934.

[106] R.P.K. Poudel, S. Liwicki, and R. Cipolla, "Fast-scnn: Fast semantic segmentation network," in *Proc. British Machine Vision Conference (BMVC)*. BMVA Press, 2019, pp. 187.1–187.12, doi: 10.48550/arXiv.1902.04502.

[107] C. Campos, R. Elvira, J.J.G. Rodríguez, J.M.M. Montiel, and J.D. Tardós, "Orb-slam3: An accurate open-source library for visual, visual–inertial, and multi-map slam," *IEEE Trans. Robot.*, vol. 37, no. 6, pp. 1874–1890, 2021, doi: 10.1109/TRO.2021.3075644.

[108] D. Fox, W. Burgard, and S. Thrun, "The dynamic window approach to collision avoidance," in *Proc. IEEE International Conference on Robotics and Automation (ICRA)*, 1997, pp. 23–29, doi: 10.1109/100.580977.

[109] M. Werling, J. Ziegler, S. Kammel, and S. Thrun, "Optimal trajectory generation for dynamic street scenarios in a frenet frame," in *Proc. 2010 IEEE International Conference on Robotics and Automation (ICRA)*, 2010, pp. 987–993, doi: 10.1109/ROBOT.2010.5509799.

[110] A. Nasrallah *et al.*, "Ultra-low latency (ull) networks: The ieee tsn approach," *IEEE Commun. Surv. Tutor.*, vol. 21, no. 1, pp. 88–145, 2019, doi: 10.1109/COMST.2018.2869350.

[111] R. Szeliski, *Computer Vision: Algorithms and Applications*, 2nd ed. Springer, 2022.